

Fiber-lasers for ultrafast optics

M.E. Fermann, A. Galvanauskas, G. Sucha, D. Harter

IMRA America, Inc., 1044 Woodridge Ave., Ann Arbor, MI 48105
(Fax +1-313/930-9957)

Received: 7 March 1997/Revised version: 16 April 1997

Abstract. The current status of a fiber-based ultrafast technology is reviewed. Pulse generation techniques capable of producing femtosecond pulses are discussed. Here we describe passive and active-passive mode locking techniques as well as linear and nonlinear fiber amplifiers. Thirty-femtosecond pulses may be generated directly from fiber oscillators or by implementing pulse compression techniques. The use of cladding-pumping and all-fiber chirped-pulse amplification allows the generation of W-level average powers from conceptually simple fiber laser systems. Nonlinear frequency conversion in highly nonlinear crystals allows a significant extension of the accessible wavelength range. Electronically phase-locked fiber lasers with unprecedented timing accuracy may be constructed by exploitation of the low-noise properties of fiber lasers. In turn, the high timing accuracy possible with fiber lasers enables the demonstration of electronic scanning delay lines for all-electronic pump-probe experiments.

PACS: 42.60.Da; 42.60.Fc; 42.80

Optical fibers have been viewed as a very attractive medium for the generation and manipulation of ultrafast pulses for a long time. Notably, the realization of fiber based pulse compression [1], and the prediction [2] and demonstration [3] of soliton propagation in optical fibers helped to firmly establish optical fibers in the realm of ultrafast technology [4–6]. However, initially the development of a comprehensive fiber-based ultrafast technology was not possible due to the lack of a fiber-based gain medium. Only with the fabrication of rare-earth-doped fibers [7, 8] have wide-bandwidth fiber gain media become readily available in a large part of the optical spectrum, stretching nearly continuously from 380 nm [9] to 3.9 μm [10]. As part of these efforts, erbium-doped fiber amplifiers (EDFAs) have been developed [11, 12] which are now firmly established in optical telecommunication systems [13] and are one of the most widely used gain media in current laser technology.

The high quality and low pump-power requirements of these wide-bandwidth gain media also sparked efforts to-

wards the construction of short-pulse fiber lasers [14], which finally resulted in the demonstration of femtosecond passively mode-locked fiber oscillators by a variety of Kerr-type [15–18] or semiconductor saturable absorbers [19, 20]. Despite the fact that with rare-earth-doped fibers a simple solid-state femtosecond laser finally became a reality, ultrafast technology continued to advance mainly around ultrafast bulk solid-state lasers, such as the Ti:sapphire laser, which became available at nearly the same time [21]. Initially, Ti:sapphire lasers turned out to be much more versatile in the field of ultrafast optics compared with fiber lasers due to their compatibility with a variety of bulk-optics pulse manipulation techniques and the much higher power levels obtainable. For example, the high extractable average power levels ($> 1 \text{ W}$) and pulse energies ($> 10 \text{ nJ}$) from Ti:sapphire lasers were employed towards the construction of widely wavelength-tunable ultrafast laser systems by way of direct pumping of optical parametric oscillators [22]. Equally, chirped-pulse amplification (CPA) techniques [23] boosted the power levels of high-repetition-rate compact Ti:sapphire amplifiers into the region of 0.1 TW [24, 25], sufficient to generate X-rays.

However, as industrial applications of ultrafast optics proliferate, the wide distribution of these more conventionally constructed systems is affected by their limited potential for integration. Only highly integrated ultrafast lasers can potentially address the needs of industrial systems due to their reduced footprint, their simplified assembly, and their high reliability arising from a compact setup. For any such technology to be widely accepted, it is also imperative that a high degree of flexibility be preserved, i.e. a large range of applications should be possible, just as with bulk-optics lasers. Clearly, fiber lasers are ideally suited in this regard, and due to the great advancements achieved during the last few years, a highly integrated, fiber-based ultrafast technology has indeed become a reality.

In this paper we will limit our review to recent work on ultrafast fiber lasers and some of their applications. An early review of ultrafast fiber lasers can be found in [14] and [26]. In Sect. 1 we discuss some of the fundamental physical limitations of optical fibers. In Sect. 2 we describe recent advances in low-peak-power fiber-based pulse sources. Sect. 3

deals with chirped-pulse amplification systems for the construction of high-power fiber laser pulse sources. In Sect. 4 we review some of the recent work on frequency-conversion techniques. And finally Sect. 5 deals with timing stabilization techniques.

1 Fundamentals

To preserve a high degree of flexibility, an integrated ultrafast laser system should offer the potential for generation of high average power levels as well as high pulse energies. The extractable pulse energy from a fiber amplifier is governed by the saturation energy given by

$$E_{\text{sat}} = \frac{h\nu A}{\sigma}, \quad (1)$$

where h is the Planck constant, A is the fiber cross-section and σ is the stimulated emission cross-section. The maximum usable core diameter for single-mode optical fibers to date is about $17 \mu\text{m}$ [27], whereas for an aluminosilicate fiber, $\sigma = 4 \times 10^{-21} \text{cm}^2$ [28], which gives a saturation energy of about $72 \mu\text{J}$. Hence the saturation energy of optical fibers is more than six orders of magnitude larger than possible in semiconductor lasers. Note that energy levels up to $160 \mu\text{J}$ have indeed been extracted from single-mode fibers with 10-ns seed pulses [27, 29]. When using femtosecond seed pulses in conjunction with chirped-pulse amplification, energy levels up to $12 \mu\text{J}$ have been generated [30, 31].

It is also instructive to evaluate the fundamental limitations for the generation of high cw power levels from fiber lasers. By employing cladding pumping, cw power levels up to 10 W have recently been obtained from Nd-doped fibers [32]. Particularly low power limitations arise when applying dielectric coatings to the ends of optical fibers. For example, a typical dielectric coating can sustain cw power intensities up to $5 \text{MW}/\text{cm}^2$, which corresponds to a cw power of only about 4 W for a $10\text{-}\mu\text{m}$ -diameter core. A higher damage threshold is expected when uncoated fiber ends are employed. Cw mode-locked Nd:YAG lasers producing 80-ps pulses with average power levels up to 8 W have indeed been coupled into uncoated fiber ends [33]. In general, the bulk breakdown threshold is expected to be at least an order of magnitude higher than surface breakdown [34]. Thus, even higher powers can be sustained by using fiber ends that have been tapered to larger diameters.

The maximum pump power that can be applied to an optical fiber is also governed by thermal limitations [34]. However, since the absorption per unit length in a double-clad single-mode fiber can be made very small, typically only thermal birefringence is a relevant factor in high-power fiber lasers. Any amount of thermal birefringence can then easily be compensated for by appropriate bending of the optical fiber.

More serious power limitations arise from stimulated Raman scattering in optical fibers. The threshold power P_{th} for stimulated Raman oscillation in an optical fiber resonator is reached when the Raman gain exceeds the resonator loss, i.e.

$$P_{\text{th}} > \frac{A}{g_{\text{r}}} \alpha_{\text{r}}, \quad (2)$$

where A is the fiber core area, α_{r} is the effective loss coefficient at the Raman wavelength and g_{r} is the Raman gain coefficient. Assuming a fiber oscillator of 100 m length with an uncoated fiber end with a reflectivity of 4% as the output coupler, we obtain an effective loss coefficient of $\alpha_{\text{r}} = 0.016/\text{m}$. For a core diameter of $7 \mu\text{m}$ and a Raman gain coefficient $g_{\text{r}} = 9.2 \times 10^{-14} \text{m}/\text{W}$ at $1.064 \mu\text{m}$ [35], we obtain $P_{\text{th}} = 6.7 \text{W}$. Higher Raman thresholds could be achieved by providing for differential loss between the signal and Raman wavelength.

The threshold for stimulated Brillouin oscillation is given by

$$P_{\text{th}} > \frac{A}{g_{\text{B}}} \frac{\Delta\nu_{\text{B}}}{\Delta\nu_{\text{s}}} \alpha_{\text{B}}, \quad (3)$$

where g_{B} is the Brillouin gain coefficient $g_{\text{B}} = 4 \times 10^{-11} \text{m}/\text{W}$ at $1.064 \mu\text{m}$ [35] and $\Delta\nu_{\text{B}}/\Delta\nu_{\text{s}}$ is the ratio between the linewidth of the Brillouin gain spectrum and the linewidth of the spectrum at the signal wavelength. For typical silica fibers, $\Delta\nu_{\text{B}} = 30 \text{MHz}$. For a cw resonator with the same parameters as before and a line width of 1 nm, we obtain $P_{\text{th}} = 136 \text{W}$. Thus stimulated Brillouin scattering is relevant only in the construction of narrow linewidth lasers.

2 Low-power fiber pulse sources

2.1 Passively mode-locked fiber oscillators

For the generation of the shortest possible pulses from a relatively simple system, passively mode-locked fiber oscillators are still the lasers of choice. By now, pulses of the order of 100 fs have been obtained from a variety of gain media, such as Nd [15], Yb [36], Er [17], Er/Yb [37], Pr [38] and Tm [39]. Early short-pulse oscillators were based on relatively complicated cavities using the all-optical switching action in nonlinear amplifying loop mirrors (NALMs) [15, 17], whereas recent work has concentrated mainly on simpler designs relying on short-pulse formation induced by nonlinear polarization evolution [16, 18, 36–39]. Alternatively, very simple short-pulse oscillators based on semiconductor saturable absorbers have also been greatly advanced [19, 20, 40, 41].

In nonlinear polarization evolution, a differential excitation of the two polarization eigenmodes of a single-mode optical fiber is used to produce an intensity-dependent phase delay between the polarization eigenmodes via the optical Kerr effect [16]. By an appropriate control of the polarization state in the fiber and by the insertion of a polarizer into the cavity, an all-optical switching action is obtained. Such devices can be constructed in both Fabry–Perot [16] and ring cavities [18] as shown in Fig. 1a,b. Due to the enhanced sensitivity of a standing-wave cavity to intracavity spurious reflections [42], the Fabry–Perot cavity typically also requires a saturable absorber for the initiation of short-pulse formation [37]. To date the shortest pulses generated from an Er fiber ring cavity are about 80 fs [43]; an Nd-fiber Fabry–Perot cavity has generated pulse widths down to about 30 fs [44].

These pulses are close to the bandwidth limit of the respective gain media and can typically only be obtained by an appropriate use of dispersion compensation in the cavity, either by implementing bulk-optics dispersion compen-

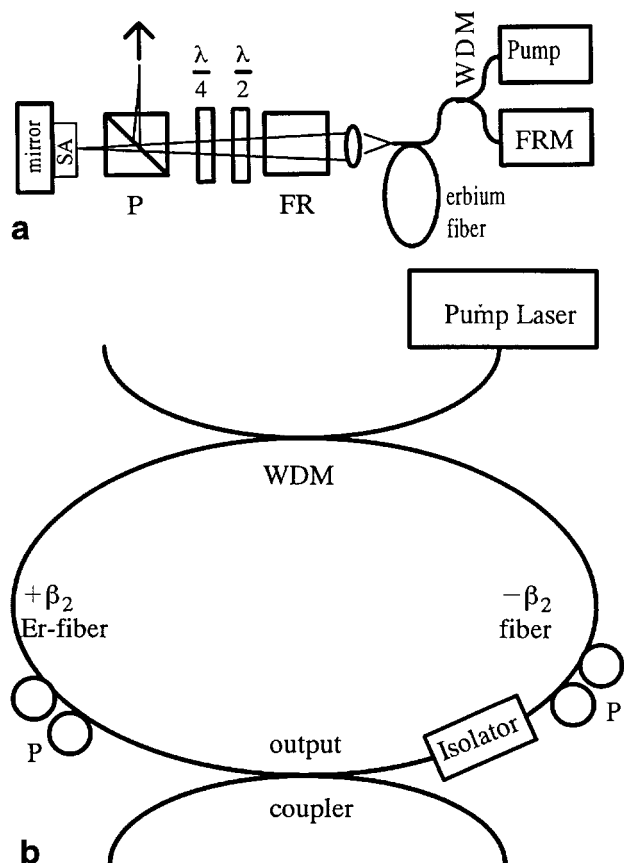


Fig. 1. **a** Typical cavity arrangement for an environmentally stable Er fiber laser. SA, saturable absorber; P, polarizer; $\lambda/2$, $\lambda/4$, half-wave and quarter-wave plates; FR, Faraday rotator; FRM, Faraday rotator mirror. **b** Typical cavity arrangement for a stretched-pulse erbium fiber ring laser. $-\beta_2$, negative dispersion fiber; $+\beta_2$, positive dispersion fiber. The isolator ensures unidirectional operation

sation [15, 16, 36, 44] or fibers with both positive and negative dispersion [18, 43]. In such oscillators, the intracavity pulse width is continuously stretched and recompressed by the large amount of linear dispersion in the cavity. In the case of bulk-optics dispersion compensation, the term “additive pulse compression mode locking” has been used for this type of laser [15], whereas in the case of all-fiber dispersion compensation, the term “stretched pulse additive pulse mode locking” has been used [18]. Due to the large dispersive perturbations of the pulses in such lasers, the pulses can be strongly chirped inside the resonator (similar to chirped-pulse amplification [23]), which in turn reduces the peak power and greatly increases the extractable pulse energy. In fact, pulse energies up to 3 nJ have been extracted from such lasers [45].

The advantage of a Fabry–Perot cavity is that it can be easily upgraded for cladding pumping as shown in Fig. 2 [37]. Passively mode-locked cladding-pumped Er/Yb fiber lasers have generated 100-fs pulses at average powers up to 15 mW at repetition rates of 50 MHz [46]. A typical autocorrelation trace and the corresponding pulse spectrum of pulses generated from such a laser are shown in Fig. 3. Cladding-pumped fiber lasers allow a very high degree of integration. However, the cavity shown in Fig. 2 may suffer from polarization

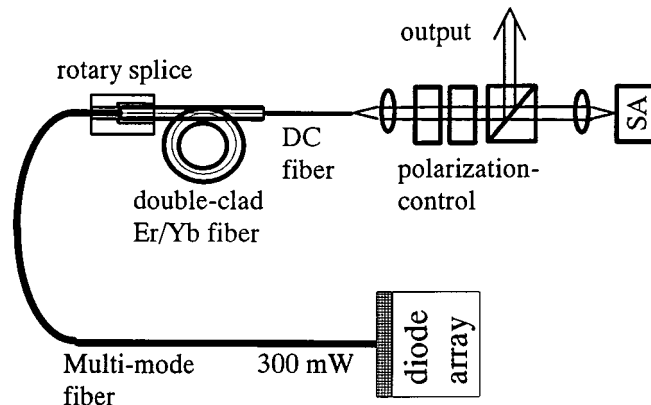


Fig. 2. Example of a cladding-pumped femtosecond oscillator based on Er/Yb fiber

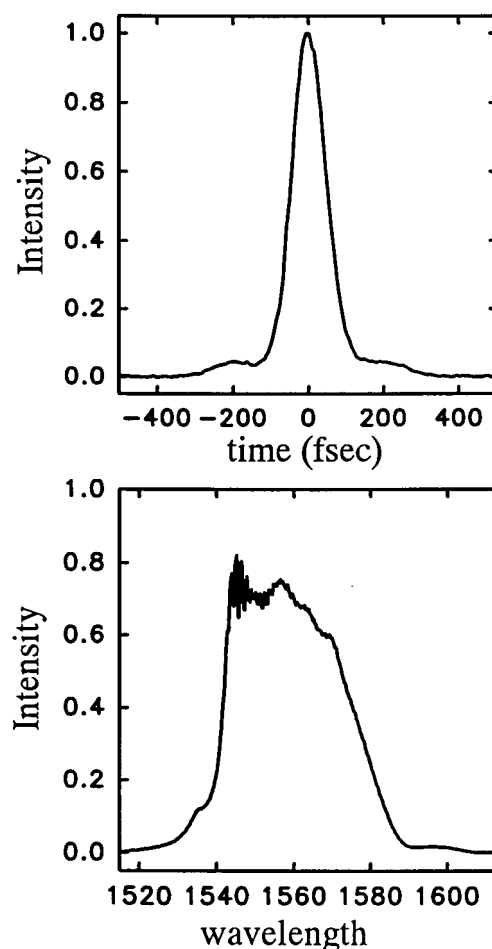


Fig. 3. Autocorrelation (*top*) and spectrum of ≈ 100 -fs pulses generated at a repetition rate of 50 MHz from the oscillator shown in Fig. 2

fluctuations, which can be eliminated by resorting to an environmentally stable cavity design [47], as shown in Fig. 1a.

As an alternative to passively mode-locked fiber lasers based on fast all-optical switching, fiber lasers may also be constructed based on semiconductor saturable absorbers. Particularly attractive are completely integrated designs. Recently, stable ultrafast pulse generation has indeed been reported in integrated Nd [40], Er [41], and Tm [48] fiber lasers.

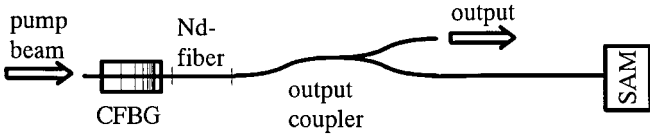


Fig. 4. Example of a fully integrated passively mode-locked Nd-fiber laser. A chirped-fiber Bragg grating (CFBG) is used for dispersion compensation. The saturable absorber mirror (SAM) is butted directly to a fiber end

These lasers consist just of a piece of fiber, a mirror, and a butt-coupled saturable absorber. The output can then also be extracted directly in form of a fiber pigtail by incorporating a coupler into the cavity [40] or by butt-coupling an external wavelength division multiplexing (WDM) coupler to the passive cavity mirror [41]. An example of an integrated fiber laser is shown in Fig. 4. Due to the lack of an ultrafast Kerr nonlinearity, the pulses from such lasers are typically longer compared with polarization-switched lasers. Also, due to a lack of polarization control in such cavities, polarization instabilities may arise [40].

Fiber lasers operating in the soliton-supporting dispersion regime of silica fibers mode-locked by saturable absorbers closely resemble true soliton lasers, where the pulse width is given simply by

$$\tau = \frac{3.53\beta_2}{\gamma W}, \quad (4)$$

where β_2 is the cavity dispersion, W is the pulse energy, and γ is the nonlinearity parameter of the fiber given by $\gamma = 2\pi n_2/\lambda A$ and n_2 ($n_2 = 3.2 \times 10^{-20} \text{ m}^2/\text{W}$ in silica glass) is the nonlinear refractive index, λ is the laser wavelength, and A is the fiber core area. The maximum oscillating pulse energy is then obtained by assuming that a maximum nonlinear phase delay of about π can be sustained by the cavity before the laser becomes unstable.

The maximum sustainable pulse energy in a passively mode-locked soliton fiber laser can be raised by greatly increasing the cavity dispersion by the incorporation of a chirped-fiber grating [49]. Wide-bandwidth highly dispersive chirped-fiber Bragg gratings are indeed easily manufacturable [50] and can be readily incorporated as one of the cavity mirrors into a fiber cavity, as shown in Fig. 4. Thus the dispersion D_2 of a cavity of length L incorporating just a few meters of fiber will be completely governed by the dispersion D_2 of the chirped-fiber grating. The pulse energy then scales with $\sqrt{|D_2|}/L$, whereas the pulse width scales with $\sqrt{|D_2|}$. Using this technique, pulses with widths of 4 ps and energies up to 10 nJ have been obtained directly from fiber oscillators [51]. Moreover, as chirped-fiber gratings allow the incorporation of negative amounts of dispersion in the whole transparency range of silica fibers, in principle compact soliton fiber lasers can be constructed in conjunction with any rare-earth fiber gain medium, as was recently demonstrated using Nd as the fiber gain medium [40, 52].

2.2 Passive harmonically mode-locked fiber lasers

Whereas the benefit of fiber lasers mode-locked at the fundamental repetition rate lies in maximizing the obtainable pulse energies while still preserving a simple cavity design, passive harmonically mode-locked fiber lasers are very useful in scaling up the obtainable pulse repetition rates.

Passive harmonic mode locking was discovered by Grudin et al., who observed that once the pump power to a soliton fiber laser is raised beyond the stability limit, under certain conditions the fiber laser can generate a multiple of equal-amplitude solitons [53]. The pulses are subject to a variety of forces due to effects such as spurious reflections, short-range soliton interactions, continuum-mitigated soliton interactions, and acousto-optic interactions. It is now widely believed that particularly long range acousto-optic interaction can lead to the self-stabilization of a passive harmonically mode-locked fiber laser [53–55]. The idea is that each soliton excites an acoustic wave which leads to a long-lived refractive index perturbation $\delta n(t)$ in the fiber. The time-varying index perturbation leads in turn to a frequency perturbation and an effective repulsive force between two subsequent solitons.

A particularly stable operation of these lasers is possible when the pulse separation in the soliton pulse train corresponds to a resonance frequency of the acoustic waves, which is typically around 500 MHz [54]. However, as the induced refractive index perturbations are very small (even in resonance the index perturbation is only of the order of 10^{-7} to 10^{-8}) and are subject to acoustic resonances of the fiber, the pulse repetition rates obtainable from passive harmonic mode locking are quite unpredictable and sensitive to cavity perturbations [55]. Further, spurious cavity reflections can prevent the laser from operating in a passive harmonically mode-locked regime.

Recently Grudin et al. suggested [56] that a similar long-range repulsive force can be obtained from phase effects in saturable absorbers; i.e. the decay of the free carriers in the absorber excited by an optical pulse leads to a phase modulation, which leads to pulse repulsion in negative dispersion fiber. From the carrier dynamics in the saturable absorber, the frequency modulation $\delta\omega$ induced by the saturable absorber is calculated as

$$\delta\omega = -\frac{\omega d}{c\tau_c} \delta n \exp\left(\frac{-t}{\tau_c}\right), \quad (5)$$

where d is the thickness of the saturable absorber, τ_c is the carrier lifetime, and δn is the peak refractive index change induced by the optical pulse.

Passive harmonic mode locking is compatible with both cladding pumping [57] and integrated cavity designs [58, 59]. In fact, an integrated fiber laser has recently produced repetition rates up to 2.5 GHz by using passive harmonic mode locking [59]. A cladding-pumped version of a passive harmonically mode-locked fiber laser has produced a pulse jitter of 50 ps at repetition rates around 100 MHz [57]. In an integrated system operating at repetition rates of 2.5 GHz, the pulse jitter could recently be reduced to as low as 1 ps in a 1-kHz bandwidth [59], though at present it is not clear whether acousto-optic interactions or the saturable absorber were responsible for the low pulse jitter.

2.3 Active-passive mode locking

Another way to obtain high-repetition-rate femtosecond pulses is to incorporate active-passive mode locking, a technique that has advanced significantly during the last few years. Active-passive mode locking schemes rely on soliton pulse-shaping in actively mode-locked lasers [60–62]. In the presence of large amounts of negative dispersion, a short soliton

pulse can be sustained, whereas the accompanying dispersive wave is spread dispersively in time sufficiently quickly to be suppressed by the active mode locker [63]. This concept has also been extended to mode locking with semiconductor saturable absorbers [64]. It was shown by Kärtner et al. [63] that in the presence of large amounts of negative dispersion, the obtainable pulse width can be decreased by a factor R below the value given by the standard Kuizenga and Siegmann theory [65], in which

$$R \leq 1.37 \sqrt{\frac{\beta_2 L}{g/\Omega_g^2}}, \quad (6)$$

where β_2 is the fiber dispersion, L is the cavity length, g is the steady-state gain, and Ω_g is the gain bandwidth. Typically, pulse widths of the order of 1 ps can be obtained at repetition rates of 20 GHz [66, 67], pulses as short as 630 fs were recently obtained at a repetition rate of 5 GHz [68].

Note, however, that these high-repetition rates can only be obtained by implementing harmonic mode locking. Due to the long relaxation times of fiber lasers, the laser will only saturate with respect to the average laser power and not individual pulses [69]. Thus, harmonically mode-locked lasers can suffer considerable pulse-to-pulse instabilities and the presence of supermodes in the radio frequency RF spectrum, which result in sidebands at the fundamental cavity round-trip time.

A large degree of supermode suppression was achieved by implementing mechanisms which can limit the pulse energy of individual pulses in the generated pulse train. Here either the incorporation of nonlinear polarization evolution [67, 69] or the use of an intracavity filter [66] were shown to provide an all-optical pulse-limiting mechanism. Note that strong all-optical limiting mechanisms were also observed in passively mode-locked and passive harmonically mode-locked fiber lasers [57].

2.4 Femtosecond pulse sources based on compression schemes

Perhaps one of the biggest attractions of optical fibers is the relative ease with which pulse compression techniques can be applied towards the construction of ultrafast pulse sources. Pulse compression techniques allow the pulse-width limitations set by the gain bandwidth of fiber laser oscillators to be overcome. Indeed, recently pulses as short as 4.9 fs have been obtained from a fiber compressor in conjunction with a femtosecond Ti:sapphire laser [70].

We can distinguish between compression schemes operating in the positive, zero, and negative dispersion regimes. Pulse compressors operating with positive dispersion fiber rely on the interplay of self-phase modulation and dispersion to broaden the bandwidth of the optical pulses and to create a linear pulse chirp, which can then be recompressed using bulk-optics dispersive delay lines [1, 33, 71]. Recently the availability of fiber gratings has allowed the construction of all-fiber varieties of such systems by implementing chirped-fiber Bragg gratings as all-fiber dispersive delay lines [72, 73]. Single-stage compression factors of the order of 10 with more than 80% of the pulse energy in a compressed 200-fs pulse have been demonstrated [72]. Particularly, high-quality

pulses can be expected by implementing positive dispersion fibers with gain in the spectral-broadening stage [74].

Fibers with nearly zero dispersion for pulse compression have been used widely to provide ultra-wide-bandwidth ‘continuum’ optical sources in optical fibers. The quasi-continuum can extend up to 200 nm in wavelength and is formed by an interplay of self-phase and cross-phase modulation as well as four-wave mixing and stimulated Raman scattering [75–77]. Note that previously very broad bandwidth sources had also been generated using multiple Raman soliton formation in optical fibers [78]; however, only the use of near-zero dispersion fibers has produced a broadband source with a high degree of symmetry with respect to the pump wavelength. Quasi-continuum sources can be readily diode-pumped and allow the generation of femtosecond pulses simultaneously at different wavelengths by implementing simple frequency filtering [77]. Successful applications of these sources in high-density WDM applications in telecommunications have also been demonstrated [79].

In the negative dispersion regime, higher-order soliton formation [80], Raman-soliton formation [80–82], and adiabatic soliton compression [83] have all been used to compress pulses in erbium-doped fiber amplifiers. Pulse widths as short as 30 fs have been obtained from a combination of Raman-soliton formation and higher-order soliton compression [84]. This design has the advantage that no external dispersive delay lines are required. Further, erbium-doped negative dispersion fiber amplifiers can be used for Raman-soliton generation, which allows for simultaneous amplification and compression. Richardson et al. have demonstrated the generation of pedestal-free 90-fs Raman soliton pulses with a pulse energy of 2 nJ at repetition rates of a few megahertz, where a compression factor of 6 was obtained [82].

In adiabatic soliton compression [85], the soliton is adiabatically amplified along the fiber so as to prevent the formation of a pedestal that typically forms when using Raman soliton and higher-order soliton compression. Alternatively, adiabatic soliton compression can be obtained by using fibers with decreasing dispersion and core area, since for a constant pulse energy the soliton pulse width is proportional to the product of fiber dispersion and core area. It can be shown by a transformation of the nonlinear Schrödinger equation that these cases are indeed equivalent [85]. Recently, adiabatic soliton compression was obtained by using amplifier fibers with dispersion-decreasing fiber [86]. For the adiabaticity condition to be fulfilled, the breakup of the fundamental $N = 1$ soliton has to be prevented. Thus the gain and the variation in fiber parameters per soliton period should be $\ll 1$.

The implementation of adiabatic soliton compression in erbium-doped dispersion-decreasing fiber has allowed the construction of wide-bandwidth gigahertz pulse sources for WDM applications [87, 88]. Compared with the supercontinuum sources, the spectral power density as well as the pulse quality can be greatly improved, albeit with a significantly smaller extent of the spectrum.

Adiabatic fiber compression and pulse-shaping techniques allow a whole range of different ultra-short-pulse sources to be made. In particular, the output from a single cw laser source can be phase- [89] or amplitude-modulated [90, 91] and then nonlinearly compressed to a high-quality pulse train at frequencies up to six times the modulation frequency by optically filtering out the higher-order sidebands from the

modulated signal [89]. Indeed, it was demonstrated that such pulse sources are useful for high-density time-division multiplexing application in telecommunication. Equally, pulse trains with repetition rates of several hundred gigahertz can be generated using the sinusoidal beat signal generated by two cw lasers with a close frequency separation for seeding an adiabatic pulse compressor [92–94]. The use of two separate lasers has not seen much further development due to the inherent jitter problems of such sources arising from the large-frequency bandwidths of the cw lasers.

More generally, nonlinear fiber compression techniques also allow the use of simple gain-switched diodes for the generation of femtosecond pulses [95]. Pulses shorter than 200 fs have been obtained from such a system [96]. Due to the inherent limited pulse quality of gain-switched diodes, rather complex multiple compression stages may be required, however.

2.5 Other pulse sources

For completeness we mention briefly a few other advances in low-power ultrafast fiber laser sources that have not yet found wide application. A phase-insensitive passive additive pulse mode-locked (APM) laser using a coupled-fiber laser cavity with three fiber gratings was recently demonstrated. Here the APM laser sets its own phase for optimum mode locking by way of passive selection of the oscillating wavelength [97].

Sliding-frequency soliton fiber lasers have been demonstrated, where cw oscillation is inhibited by suppression of longitudinal cavity modes by the incorporation of a continuous-frequency shifter into the cavity [98, 99]. Due to the ability of soliton pulses to follow small-frequency perturbations, a soliton train may still be trapped in the presence of an optical filter, whereas cw lasing is suppressed. Indeed, soliton pulses at repetition rates of several gigahertz have so been generated. All-fiber sliding-frequency sources of ultrashort pulses have also been constructed using all-fiber frequency modulators [100, 101].

Further progress has been reported in short-pulse sources based on frequency-swept semiconductor lasers. This technique sweeps the oscillation frequency of a distributed Bragg reflector DBR [102] or a twin-guide laser [103] electronically across a wavelength range of up to 10 nm in a subnanosecond or nanosecond time period. The frequency chirp of these long pulses can be linearly compensated in a long-length fiber [102] or in a fiber grating [104]. Advantages of this technique include the possibility of external triggering, high repetition rates (up to 0.5 GHz has been demonstrated [103]), and low timing jitter (less than 100 fs [103]). The use of higher-order soliton compression has also allowed the generation of pulses as short as 230 fs [102]. Using adiabatic soliton compression, 540-fs-duration pulses with low pedestal have been achieved [105].

Finally, advances have also been reported in the generation and detection of dark-soliton pulse trains. In one experiment, positive-dispersion-decreasing fiber has been used to generate dark soliton pulses at 100-GHz repetition rates from the sinusoidal beat signal of two single-frequency distributed feedback DFB lasers [106, 107]. In another experiment grey optical solitons have been generated in an optically mode-locked fiber laser [108]. A method for generating and

detecting dark solitons compatible with standard data generation techniques in optical communications has been described by Nakazawa et al. [109]. Here, dark pulses are generated by direct modulation of a single-frequency laser. At the detection end, an interferometric combination of the pulse train with a one-bit shifted replica of itself creates an inverted non return-to-zero NRZ format carrying the information from the dark solitons. Nakazawa et al. have also demonstrated the application of dark solitons in long-distance communication [110]. Clearly, whereas dark solitons have been proven to be a viable alternative to bright pulses in the field of telecommunications, dark pulses play no role in the application of ultrashort pulses discussed in the following chapters.

3 Fiber-based chirped-pulse amplification systems

The general problem encountered when directly amplifying ultrashort optical pulses is that unacceptably high peak intensities are easily reached at pulse energies well below the maximum attainable energies, as determined by the saturation fluence value and the energy storage capacity of a particular gain medium. High peak intensities are associated with nonlinear pulse-shape distortions and optical damage of the components. One way to alleviate the problem is to expand the transverse dimensions of the propagating beam, the gain medium, and all the optical components in order to reduce the peak intensities. Unfortunately, this leads to an unacceptable dramatic increase in the size of the laser system, limiting the practicality of this approach. Chirped-pulse amplification (CPA) is a more elegant and practical solution to the problem of amplifying ultrashort pulses [23]. By virtue of their large spectral bandwidth, ultrashort pulses can be substantially stretched in length rather than in the transversal spatial dimension, thus reducing the peak intensities to acceptable levels. For solid-state lasers the implementation of CPA has led to the development of tabletop TW peak-power systems [24, 25, 111].

CPA is essential for the amplification of ultrashort optical pulses in a fiber gain medium due to its small transversal dimensions and long propagation lengths. Direct amplification of undistorted femtosecond pulses is not possible for pulse energies above the ~ 1 -nJ level [80, 112], while the energy extraction potentials of a fiber amplifier are substantially higher than this, allowing for maximum pulse energies in the 100- μ J range [27]. Considering that femtosecond fiber oscillators can only produce pulse energies up to the nanojoule level, the importance of CPA for bridging this energy gap is obvious.

The particular feature of using CPA in conjunction with fiber technology is that the compact size typical of fiber amplifiers necessitates the development of compact alternatives to diffraction grating-based dispersive delay lines (DDL), traditionally used for pulse stretching and recompression. The task is greatly facilitated by the fact that the pulse energies specific to fiber amplifiers can be substantially smaller than those from solid-state CPA systems [23–25, 111]. Use of chirped in-fiber gratings as DDLs is one such solution suitable for a certain energy range [113]. The essential advantage of fiber gratings is that they are ideally compatible with fiber amplifier technology in terms of manufacturability, size, cost, and robustness. At present, however, the conventional

diffraction-grating DDLs are still a necessity for reaching the highest pulse energies from a fiber CPA system at approximately the microjoule level and above.

The clear-cut technological advantage of fiber-grating DDLs is the basis for differentiating the variety of fiber CPA designs into two main types: high-average-power fiber CPA and high-pulse-energy fiber CPA. The former type of fiber CPA systems rely on fiber-grating DDLs with relatively low output pulse energies in the 10- to 100-nJ range, and high repetition rates and high average output powers are characteristic for this type of design. In contrast, the use of diffraction-grating DDLs can be justified only by the need to reach the highest output pulse energies, which in general implies low pulse repetition rates and, consequently, lower average output powers. Furthermore, the distinction between these two types of fiber amplifiers include substantial differences in the geometry and design of amplifier fibers and in the pumping schemes.

3.1 High-pulse-energy systems

Obviously, the main criterion for choosing the amplifier fiber design parameters for this type of CPA system is to maximize the energy of the amplified and recompressed ultrashort pulses. There are two principal limitations. First, the maximum extractable pulse energy is determined by the saturation fluence. Also, the efficiency of energy extraction is affected by gain saturation through amplified spontaneous emission (ASE). Second, it is necessary to avoid significant phase distortions through nonlinear effects in the amplifier fiber in order to prevent the degradation of the recompressed pulse quality and duration.

Considering that the saturation fluence is linearly proportional to the signal mode size (1), it is obviously advantageous to increase the core size of the amplifier fiber. In addition, it has been suggested by Nilsson and Jaskorzynska [114] that increasing the mode size and dopant profile radius might reduce gain saturation due to ASE. Also, increasing the mode size effectively reduces distortions of the pulse phase $\Delta\varphi$ induced by self-phase modulation, which is proportional to the square of the peak intensity I : $\Delta\varphi \propto LI^2$. The latter equation also indicates that the effective propagation length L needs to be minimized, which makes fibers with maximum dopant concentrations a preferred option for high-energy CPA systems. In general, undistorted femtosecond pulse amplification requires peak nonlinear phase shifts of less than $\sim \pi$ [115].

For maintaining a single transverse mode in an optical fiber, an increase in the core size has to be accompanied by an appropriate reduction of the fiber numerical aperture (NA) [116]. However, a reduction of the NA is associated with an increase in fiber bend losses, which ultimately limits the maximum mode size. With all this taken into account, Er-doped fibers optimized for high-energy operation have been designed and fabricated [117]. The obtained core diameters are 12–17 μm with the fiber NA ranging from 0.06 to 0.08, resulting in transversal mode areas up to 230 μm^2 . This represents a near-tenfold increase compared with the 25–50 μm^2 mode areas of standard Er fibers, which are optimized for maximum small-signal gain.

The saturation fluence for such Er-doped large-core fibers yields saturation energies of $\sim 72 \mu\text{J}$. Indeed, Taverner et

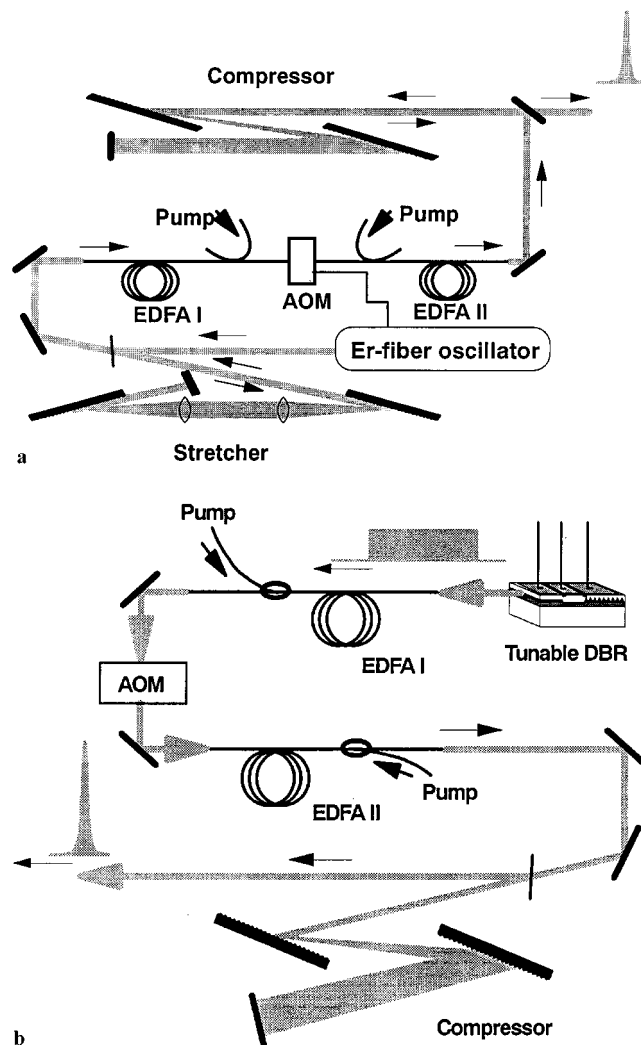


Fig. 5a,b. Basic layouts of high-pulse energy fiber CPA systems: **a** is the traditional CPA scheme with a mode-locked femtosecond source; **b** is the CPA scheme with a fast frequency-swept laser diode source

al. [27] have demonstrated 160 μJ produced by long-pulse (~ 10 ns) amplification in these large-core fibers. Unfortunately, the stretched-pulse phase distortions caused by self-phase modulation appears to be the main energy-limiting factor for a femtosecond CPA system. At present the pulse energies from large-core Er-fiber CPA systems are approximately an order of magnitude lower than the long-pulse amplification result [117]. Further increases of the energy from a CPA system require substantially longer stretched pulses than those currently available with conventional diffraction-grating DDLs.

The basic layouts of high-pulse-energy fiber CPA systems are shown in Figs. 5a,b. The essential difference here is that different types of oscillators are used. Figure 5a represents a conventional CPA scheme with a femtosecond oscillator, a Martinez-type [118] diffraction-grating stretcher, and a Treacy-type [119] diffraction-grating compressor. To minimize the size of the diffraction-grating DDL for an Er-fiber CPA system operating at ~ 1550 nm and to maximize the stretched-pulse duration, holographic gratings with 1200 lines/mm should be used. Typically, the energy-transmission of such a Treacy-type pulse compressor is about

60–75%. Figure 5b shows a hybrid scheme with a frequency-swept laser diode source [30]. The latter technique produces linearly chirped and broad-bandwidth pulses directly from a diode laser. The chirp duration and spectral width are determined by the electronic control circuits of the laser driver. There are two advantages to this CPA scheme. First, pulses can be externally triggered at any arbitrary repetition rate up to ~ 1 GHz. Second, no pulse stretcher is required, which increases the compactness of the system. However, at present only ~ 10 nm spectral bandwidth is available from such a diode, which essentially limits the output pulse duration to the picosecond range. Note that although picosecond pulses are also obtainable with gain-switched laser diodes, the limited bandwidth of gain-switched pulses (typically at ~ 1 nm) poses a serious problem for the recompression of such pulses with a diffraction-grating DDL.

Despite the differences in the oscillator and stretcher/compressor configurations, the design of the fiber amplifier itself can be identical for both systems. Considering that the seed-pulse energies are typically in the tens of picojoule range and that the maximum output pulse energies are in the tens of microjoule range, an energy gain of ~ 60 dB is required. For Er-doped fibers it is impractical to expect such a high gain from a single amplification stage. Two or three amplification stages are typical for Er-doped fiber CPA systems. For minimizing the nonlinear phase distortions, the last amplification stage is usually constructed using a short 1–2 m length of highly doped (up to 4000 ppm of Er) large-core fiber. At present, the demonstrated high-energy fiber CPA systems are in-core pumped, and therefore require up to 1 W of pump power at 980 nm from a single-mode master-oscillator power-amplifier laser diode (MOPA).

The use of acousto-optic modulators (AOM) as optical gates in multistage fiber-amplifier configurations is determined by two main reasons. First, it is necessary to prevent cross-saturation of the amplifier gain caused by cross-coupling of ASE between the different stages. Second, in order to maximize the pulse energies from the final amplification stages, it is necessary to reduce the pulse repetition rate. Typically, the pulse energies obtained from Er-doped fiber amplifiers are constant up to repetition rates of 5 to 10 kHz. This is indicated in the dependence of the measured pulse energy on repetition rate as shown in Fig. 6. The demonstrated highest pulse energy from a fiber CPA system is 14 μ J [117].

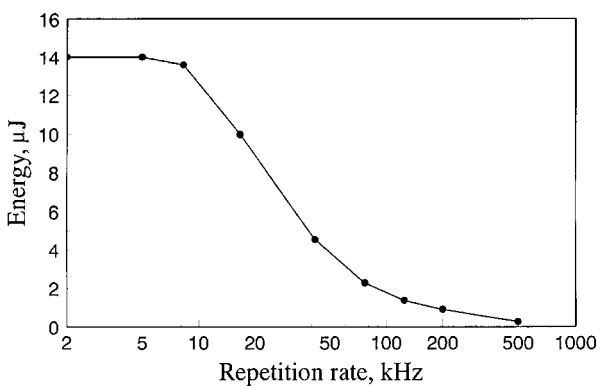


Fig. 6. Amplified pulse energy dependence on repetition rate from a high-energy Er-fiber CPA system

The pulse durations of the recompressed pulses are determined by the spectral bandwidth of the amplified μ J pulses. Due to substantial gain narrowing at 60 dB of total gain, in silica Er fibers typical recompressed pulse widths are ~ 500 fs. Pulses shorter than 300 fs have also been reached by implementing spectral manipulation techniques similar to those used in solid-state CPA systems [120, 121].

Finally, by resorting to multi-mode fibers, a substantial increase in the extracted pulse energy can be achieved. Desthieux et al. [29] reported 0.4 mJ energy extraction from a multimode Er-doped amplifier in 10-ns-long pulses. However, the requirement for high spatial and temporal coherence, which is usually associated with generating femtosecond optical pulses, limits the usefulness of this approach for a femtosecond CPA system. Nevertheless, it may still be acceptable for picosecond pulses, as was demonstrated recently. After recompression more than 100 μ J of pulse energy with picosecond pulse durations has been obtained using a 30- μ m-core multi-mode Er-fiber amplifier in the last stage [122].

3.2 High-average-power systems

The standard method of in-core pumping requires high-brightness pump sources such as single-transverse-mode laser diodes. However, the use of high-brightness laser diodes poses two essential limitations. The attainable pump powers from these sources are fundamentally limited by the maximum allowable peak intensities at the output facet of a semiconductor device. Commercially available laser diode MOPAs currently can produce up to ~ 1 W of power, which is close to the estimated technological limit. Also, the high cost of high-brightness diodes currently limits their use with fiber devices.

On the other hand, low-brightness diodes, such as broad-stripe single diodes and diode arrays can provide any required pump power in the 10- to 100-W range at low cost. By use of double-clad fiber structures [123], efficient and simple brightness conversion from high-power large-area multimode laser diode pump sources into a single diffraction-limited fiber mode can be obtained. In fact, commercial systems delivering up to 8 W of power from such sources have recently become available. Additional advantages are offered by the flexibility of different pump-coupling schemes. For example, Ripin and Goldberg [124] recently reported V-groove-assisted side pumping of a double-clad fiber, which demonstrates the potential for multiplexing several pump diodes in order to obtain high pump powers coupled into a double-clad structure.

A unique feature of high-power, fiber-based systems is the use of compact fiber grating based DDLs for pulse stretching and compression. Hence, a fiber CPA design is very different from a solid-state CPA system. One unique difference is the substantially reduced size and increased robustness of a fiber CPA system. The maximum duration τ of the stretched pulse is directly determined by the maximum round-trip delay in a chirped-fiber grating: $\tau = 2L/v_g$. Here v_g is the group velocity of light in the fiber structure and L is the grating length. For silica-glass fiber this yields ~ 100 ps/cm of delay per chirped-fiber-grating length. Current technology can produce chirped fiber gratings with lengths over 10 cm (gratings of 1 m length have even been fabricated [125]), corresponding to over 1 ns of delay. In contrast, with conventional diffraction-grating DDLs this delay could be achieved with a grating

separation of ~ 0.5 to 1 m. Note that the bandwidth of a fiber grating is solely determined by the maximum span of the grating pitch variation, and can be arbitrarily tailored according to specific needs in the range from 1 to over 100 nm. This is more than sufficient for the application of such gratings to the stretching and recompression of femtosecond optical pulses.

Another unique feature is that opposite propagation directions in a single chirped Bragg grating can be used for stretching and recompression of ultrashort optical pulses. Ultrashort pulses incident from opposite directions into a chirped-fiber Bragg grating will acquire opposite signs of the frequency chirp. An initial pulse is recompressed back if the amplified stretched pulse is reflected from the other end of the grating. The advantage here is that the effect of longitudinal irregularities is canceled out and the phase characteristics of fiber-grating DDLs are completely reciprocal for opposite propagation directions. The phase reciprocity no longer holds at high peak intensities of amplified and recompressed pulses when nonlinear effects cause additional phase distortions. This can lead to either a degradation or an improvement of the compressed pulse shape and duration. However, because the effective propagation length of the recompressed high peak power pulses is only millimeters or centimeters in a chirped-fiber grating, any nonlinear distortions of the compressed pulses are expected at significantly higher energies compared with the amplification of unstretched pulses in optical fibers. Indeed, numerical simulations and experimental studies revealed that recompressed femtosecond pulses with energies as high as hundreds of nanojoules are accessible [126].

In a germanosilicate fiber a Bragg grating can be formed in the core via a light-induced periodic refractive-index change. Using photosensitivity-enhancing techniques gratings can be written in any germanosilicate fiber, including standard telecommunications fibers [50, 127]. Fiber gratings can be directly patterned from the side of a fiber with ultraviolet light using interferometric [128] or phase-mask techniques [129]. The latter method is more attractive due to its similarity to conventional lithographic techniques used in mass-producing semiconductor integrated circuits.

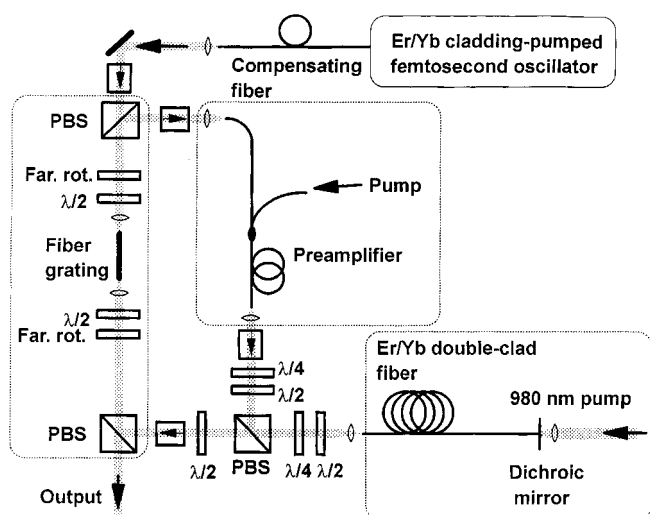


Fig. 7. Example of a high-power CPA system with a reciprocal fiber-grating dispersive-delay line

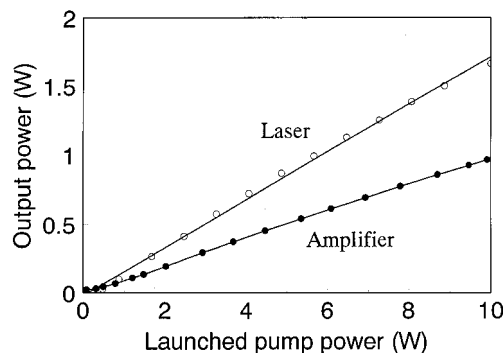


Fig. 8. The power characteristics of a double-clad Er/Yb fiber pumped with 10 W at 980 nm

One example of a high-power chirped-pulse amplification system is shown in Fig. 7 [130]. In this system both the oscillator and the power amplifier were cladding-pumped with broad-area laser diodes. The mode-locked cladding-pumped Er/Yb fiber oscillator [37] produced ~ 200 -fs bandwidth-limited pulses at a repetition rate of 18 MHz. The amplifier system consisted of a standard Er-only-doped single-mode preamplifier and a double-clad Er/Yb power amplifier. With aberration-corrected optics up to 10 W of pump power was delivered into the double-clad power amplifier. The amplifier was arranged in a double-pass configuration. The power characteristics of the double-clad Er/Yb fiber are shown in Fig. 8. The measurement in a laser configuration was obtained by using a right-angle cleaved uncoated fiber end for output coupling. The maximum output power for laser operation was 1.7 W. The maximum output power for the amplifier configuration with 20-mW signal input from the preamplifier was 1 W.

Pulse stretching and recompression for chirped-pulse amplification was accomplished with a single 10-cm-long grating with a bandwidth of 18 nm. Such long gratings provide ~ 1 ns-duration stretched pulses, which are sufficient to eliminate nonlinear interactions in a fiber amplifier even at pulse energies of ~ 1 J. The use of a single grating ensures the reciprocity of the pulse stretching and recompression stages and the generation of near-transform-limited 310-fs pulses at the output of the system (Fig. 9). Any additional negative group-velocity dispersion due to fibers in the path of the

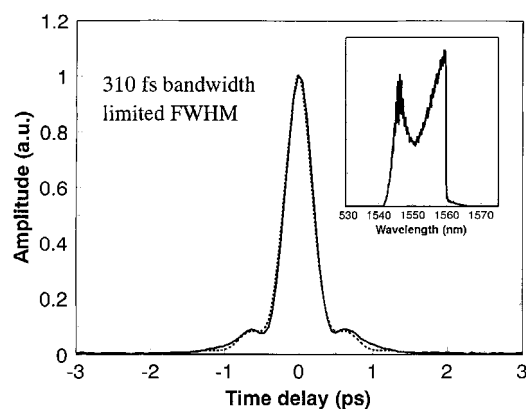


Fig. 9. Measured and calculated autocorrelation traces of 310-fs amplified and recompressed pulses from a 1 W fiber amplifier

stretched pulses is compensated for by a proper length of positive-dispersion fiber. Note the dashed-line trace in Fig. 9, which corresponds to a calculated transform-limited autocorrelation trace of the recompressed spectrum shown in the insert. It indicates the remarkable reciprocity of this stretching/compression scheme. After recompression up to 600 mW of power was extractable from this system.

4 Frequency conversion

The existing fiber gain media, suitable for mode-locked femtosecond sources, are available for certain wavelengths only within the 1- to 2- μm spectral range. For example, femtosecond fiber oscillators have been demonstrated at ~ 1064 nm [15] (Nd-doped silica glass), ~ 1300 nm [38] (Pr-doped fluoride glass), ~ 1550 nm [17, 37] (Er-doped or Er/Yb-doped silica glass), and ~ 1850 nm [39] (Tm-doped silica glass). Furthermore, all these gain media possess a limited-gain bandwidth, allowing only for narrow wavelength tuning bands (typically tens of nanometers wide). The extension of the available wavelengths beyond this spectral range (towards both longer and shorter wavelengths) is fundamentally impeded not only by the limited choice of the currently available rare-earth doped fibers but also by issues related to dispersion management within a fiber laser cavity.

This section describes the use of different nonlinear frequency conversion techniques for extending the spectral range, accessible with fiber-based femtosecond systems, and for achieving wide wavelength tunability.

4.1 Second-harmonic generation using femtosecond fiber oscillators

Second-harmonic generation (SHG) is a straightforward method to generate short-wavelength femtosecond pulses using a fiber laser. The key limitation here is that typical pulse energies from a fiber laser are relatively low, which implies a limited SHG conversion efficiency. Therefore, a careful choice of appropriate nonlinear optical materials is essential for maximizing the SH pulse energies.

A comparative analysis of various nonlinear materials for femtosecond-pulse SHG at 1550 nm has been performed by Arbore et al. [131]. The conversion efficiency η for the focussed-beam SHG in the undepleted pump limit is proportional to [132]

$$\frac{\eta}{P_\lambda} \propto \frac{d_{\text{eff}}^2 L}{n_\lambda n_{\lambda/2}}, \quad (7)$$

where d_{eff} is the effective material nonlinear coefficient, L is the interaction length, P_λ is the peak fundamental power, and n_λ and $n_{\lambda/2}$ are the refractive indices at the fundamental and second-harmonic wavelengths, respectively. The maximum interaction length for generating undistorted SH ultrashort pulses is limited by group velocity walk-off between the fundamental and second-harmonic pulses, $L_{\text{walk-off}} \propto \Delta n_g^{-1}$. Here $\Delta n_g = |n_{g,\lambda/2} - n_{g,\lambda}|$ is the group velocity mismatch between the fundamental and second harmonic. This gives a material figure of merit (FOM) for noncritically phase-

Table 1.

Material	Phase matching	FOM	Efficiency
PPLN	Noncritical	$710 \text{ pm}^2/\text{V}^2$	95 %/nJ
PPLT	Noncritical	$320 \text{ pm}^2/\text{V}^2$	43 %/nJ
LBO	Noncritical	$42 \text{ pm}^2/\text{V}^2$	6 %/nJ
KTP	Critical	$20 \text{ pm}^2/\text{V}^2$	1.5%/nJ*
BBO	Critical	$340 \text{ pm}^2/\text{V}^2$	6 %/nJ*
LiIO ₃	Critical	$12 \text{ pm}^2/\text{V}^2$	0.6%/nJ*

* 100 fs pulse assumed, spatial walk-off included

matched SHG of ultrashort pulses as

$$\text{FOM} = \frac{d_{\text{eff}}^2}{n^2 \Delta n_g}. \quad (8)$$

Note that for critically phase-matched SHG the interaction length can be limited by spatial beam walk-off rather than by temporal pulse walk-off, which has to be taken into account when calculating maximum conversion efficiencies.

Table 1 summarizes the suitability of various nonlinear materials for ultra-short-pulse SHG at 1550 nm. At the top of the list are quasi-phase-matched (QPM) materials, such as periodically poled lithium niobate (PPLN) [133] and lithium tantalate (PPLT) [134], which are one order of magnitude more efficient for ultra-short-pulse SHG compared with conventional birefringence phase-matched materials. It is a somewhat unexpected result, because QPM interaction is not phase velocity-matched, and in general, the group velocity mismatch is larger than in phase-matched interactions. These exceptionally high efficiencies are obtained through the use of the large d_{33} nonlinear tensor elements of lithium niobate or lithium, which can be utilized for SHG only through the use of QPM. The difference between the magnitude of the nonlinearity in QPM and in conventional materials is so large that it outweighs the reduced interaction length due to the larger temporal walk-off.

In practice the high FOM of PPLN allows to achieve high 10–50% conversion efficiency for fundamental pulse energies in the 100 pJ to 3 nJ range, typical for femtosecond fiber oscillators. One example of an experimentally measured conversion efficiency as a function of average fundamental power

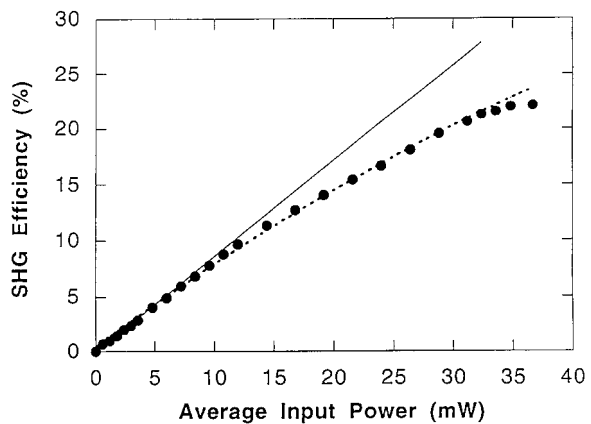


Fig. 10. Second-harmonic conversion efficiency of femtosecond fiber laser output using PPLN crystal

in a PPLN crystal is shown in Fig. 10 [131]. The 18.75-m QPM period in a z-cut wafer of a congruent lithium niobate was produced by electric field poling [135]. An Er-fiber soliton oscillator was generating 230 fs sech^2 -shaped pulses with pulse energies up to 420 pJ at a repetition rate of 88 MHz. With 37 mW of internal pump power at 1.55 μm up to 8.1 mW of SH power was generated inside the crystal. Note that each of the uncoated input and output facets of the PPLN sample have $\sim 14\%$ reflectivity losses for the pump and generated frequency-doubled light.

Spectra and autocorrelation traces of the fundamental and SH pulses are shown in Fig. 11a,b. The fundamental pulse spectrum had characteristic secondary peaks indicating the presence of a pedestal, as also seen on the autocorrelation trace (shown on a log scale). However, the high quality of the output SH pulses is indicated by the absence of this pedestal in the second-harmonic pulse spectrum and autocorrelation trace. The second-harmonic pulse duration was 190 fs with a time-bandwidth product of 0.44. Modelling of the spectrum and the autocorrelation of the frequency-doubled pulses using the nonstationary-SHG theory [136] revealed that the pulse shape was transformed from sech^2 to approximately Gaussian due to non-negligible group velocity walk-off. The observed value of the small-signal conversion of 85%/nJ is close to the predicted value of 95%/nJ [131], thus confirming the expected high SHG conversion efficiency for typical pulse energies from an Er-doped femtosecond fiber oscillator.

Note that similar conversion efficiencies can also be obtained with shorter femtosecond pulses. The bandwidth for second-harmonic generation (due to group velocity walk-

off) for PPLN scales linearly with the length of the crystal with a coefficient $\sim 12.6 \text{ nm/mm}$; also, the peak power of a pulse scales linearly with pulse duration. For example, with a 400- μm -long PPLN sample (30-nm bandwidth) 80-fs second-harmonic pulses were obtained with comparable conversion efficiencies.

The above results can be compared with frequency doubling of fiber-laser pulses in conventional birefringence-matched nonlinear crystals. Nelson et al. [45] reported a maximum conversion efficiency of $\sim 10\%$ achieved in a BBO crystal using 3-nJ pulses at 1.55 μm , which at present represent the highest pulse energies directly from a femtosecond fiber oscillator. For more typical energies below $\sim 1 \text{ nJ}$, this BBO doubler would yield unacceptably low conversion efficiencies. On the other hand, with this pump source and a 300- μm long PPLN crystal, the predicted conversion efficiencies should significantly exceed 50%, limited by the details of pump depletion and the quality of the oscillator pulses.

4.2 Fiber CPA-based tunable parametric sources

For applications which require femtosecond pulses with tunable wavelengths in the visible, near- and mid-infrared spectral regions, the universal solution is to employ parametric frequency conversion schemes, such as synchronously pumped optical parametric oscillators (OPOs) [137] or traveling-wave optical parametric generators (OPGs) [138] and amplifiers (OPAs) [139]. Such schemes, however, rely on substantial pulse energies and average powers, which are difficult to achieve from a fiber system without resorting to the above-described CPA schemes. In particular, the limited pulse energies and average powers from femtosecond fiber oscillators are currently an impediment for the direct implementation of femtosecond OPO schemes. Therefore, the first fiber laser-based source of parametrically converted wavelength-tunable femtosecond pulses was demonstrated using a high-energy fiber CPA system [140].

Due to the low repetition rate and relatively high pulse energies characteristic to a high-energy amplifier, OPG is the natural choice for parametric frequency conversion with such a system. Additionally, the advantage of an optical parametric generator compared with other parametric conversion schemes is its inherent simplicity and robustness: it does not require an optical cavity, typically associated with the need for cavity length stabilization. This simplicity is particularly compatible with the compactness of a fiber system. However, the majority of existing OPG systems require large pump energies, tens to hundreds of microjoules at least, which is at the ultimate limit for fiber-based CPA systems. This is the main reason the advantage of the simplicity of OPG was previously outweighed by the necessity to employ large and complex solid-state laser-pumping systems. Novel efficient nonlinear materials such as PPLN allow one to take full advantage of the simplicity of a single-pass OPG because of the accessibility of the required pump energies with compact fiber-based amplified sources.

The main reason for these reduced pump energies for OPG in PPLN is, as in the case of SHG, the large nonlinear coefficient d_{33} of lithium niobate accessible only through quasi-phase matching. The benefits of QPM materials in practical applications go even further. The implementation of

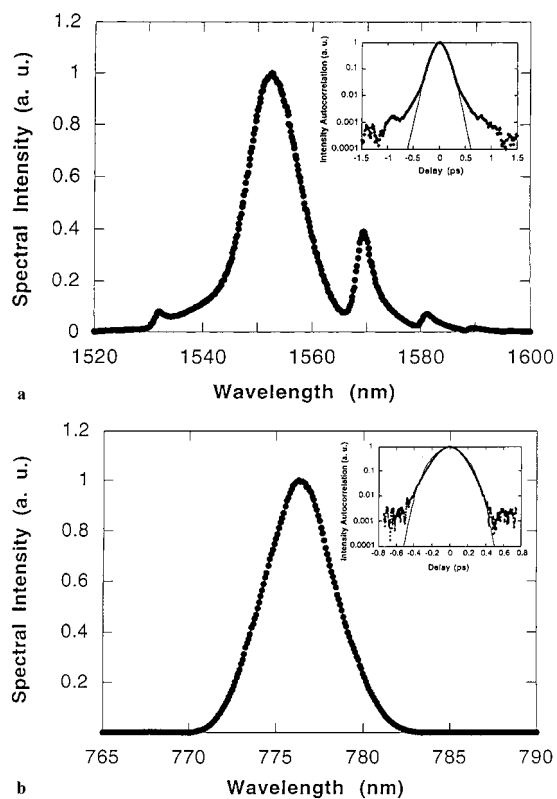


Fig. 11a,b. Spectra and autocorrelation traces of (a) the fundamental and (b) the second-harmonic pulses

QPM using conventional photolithographic techniques enables one to engineer the nonlinear properties of the crystal and, for example, to achieve phase matching of any required nonlinear interaction at any wavelength within the crystal transparency range.

The μJ -energy Er-fiber CPA source used for pumping the parametric generator in the first demonstration experiment [140] was a two-stage fiber amplifier system with a diffraction-grating stretcher and a compressor, arranged as described in the previous section on fiber CPA sources. The CPA source was producing 600-fs pulses at $1.554\ \mu\text{m}$. The OPG system was ultimately simple, consisting of a frequency-doubling crystal followed by a single-pass parametric generator crystal. When using a PPLN crystal for SHG, a maximum second-harmonic conversion efficiency of 47% (external) was achieved at saturation. The pulse energies were maximized when operating the system at 1- to 10-kHz repetition rates; after recompression, the maximum fundamental pulse energy at $1.554\ \mu\text{m}$ was $4\ \mu\text{J}$ and the maximum second-harmonic energy at $777\ \text{nm}$ was $1.9\ \mu\text{J}$.

PPLN samples of 3 mm length and 0.5 mm thickness with QPM grating periods ranging from 19 to $20\ \mu\text{m}$ were used for parametric generation. Calculated (solid curves) and measured (circles) tuning curves for the signal and idler wavelengths are presented in Fig. 12a,b. Figure 12a represents the

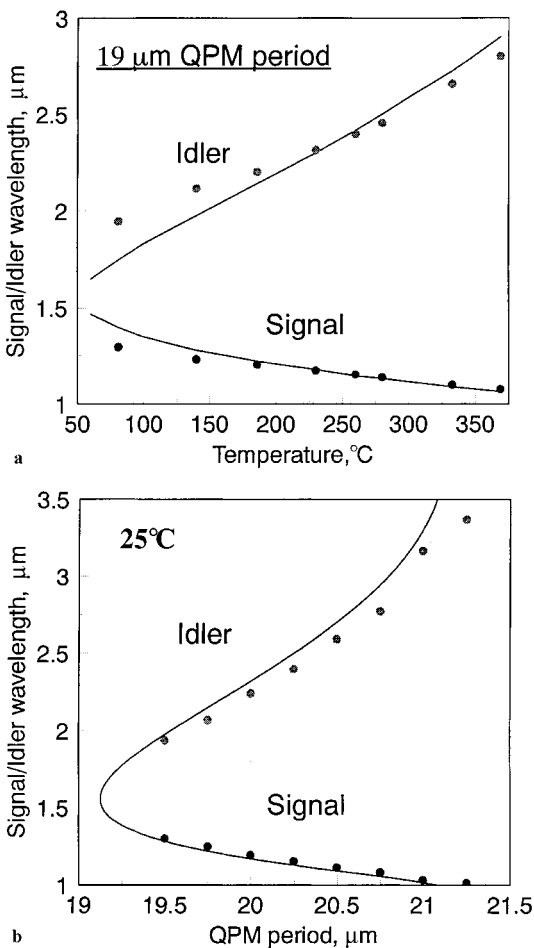


Fig. 12a,b. Tuning curves for a fiber CPA pumped optical parametric generator measured using (a) temperature tuning and (b) multigrating PPLN structure

tuning accomplished by heating the OPG crystal with a fixed $19\text{-}\mu\text{m}$ QPM-period. Changing the crystal temperature from 60 to $375\ ^\circ\text{C}$ tunes the signal wavelength from $\sim 1.4\ \mu\text{m}$ down to $\sim 1.05\ \mu\text{m}$ and the idler wavelength from $\sim 1.65\ \mu\text{m}$ up to $\sim 2.9\ \mu\text{m}$. Figure 12b shows the tuning curve measured at a fixed temperature by using a multigrating PPLN crystal. Multiple QPM gratings with different periods located on the same crystal provided steplike tuning by translating the crystal in the direction perpendicular to the beam propagation, as described in [141]. This clearly demonstrates the advantage of being able to engineer the nonlinear properties of a QPM material.

The dependence of the conversion efficiency on pump energy in a 3-mm-long sample is shown in Fig. 13. The signal wavelength for this measurement was $1.2\ \mu\text{m}$, and the pulse repetition rate was 71 kHz. The internal conversion efficiency (with energy losses at each of the uncoated facets of the PPLN crystal taken into account) is shown here. Depending on the focusing conditions, it was possible to reach either the lowest threshold (circles) or the highest conversion efficiency (diamonds). With symmetric focusing (minimum waist in the center of the crystal), the OPG threshold was $54\ \text{nJ}$ and the conversion efficiency reached saturation at $\sim 23\%$ with $100\ \text{nJ}$ of pump inside the crystal. With the minimum waist located at the back facet, the OPG threshold was $100\ \text{nJ}$ and the maximum total conversion efficiency was $\sim 38\%$, with $220\ \text{nJ}$ of pump inside the crystal. These nanojoule pump energies constitute more than an order of magnitude improvement over the best previously reported OPG pumping results ($\sim 2\ \mu\text{J}$ in [142]). The idler power was measured to be about one-third of that of the signal at $1.2\ \mu\text{m}$, consistent with photon conservation. Maximum detected signal energies of $200\ \text{nJ}$ were obtained with the maximum pump energy of $1.9\ \mu\text{J}$ at 1- to 10-kHz repetition rates. It is important to note that even at the highest pump energies no crystal damage occurred, and that the low OPG threshold allowed to operate the parametric generator at repetition rates of up to 200 kHz.

The signal pulse duration measured through SH autocorrelation was 300 fs (assuming a Gaussian pulse shape). The duration of the idler pulses is expected to be similar to that

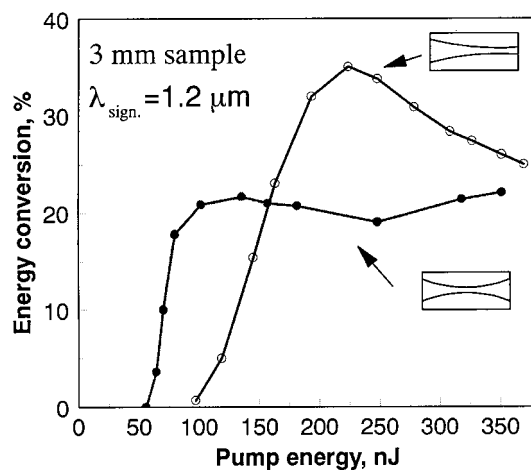


Fig. 13. Parametric conversion efficiency. Focusing conditions shown were optimized for either minimum OPG threshold or maximum conversion efficiency

of the signal, because the temporal walk-off between the idler and the signal over the entire tuning range is < 60 fs/mm, which for a 3-mm crystal is smaller than the pulse duration. The signal pulse spectrum was five to six times broader than the bandwidth limit. Non-transform-limited pulses are typical for simple single-pass OPGs. This drawback can be eliminated by resorting to more complex arrangements, such as a double-pass OPG with spectral selection [142] or a continuum-seeded OPA [139]. Note, however, that the OPG thresholds achieved are substantially smaller than typical thresholds for continuum generation. The low OPG threshold indicates that pumping of such parametric converters with a compact fiber-grating CPA system should be possible.

5 Timing and synchronization techniques

The timing of laser pulses is almost always a key issue in applications of ultrafast lasers. For many applications, such as telecommunications, short-pulse lasers must be synchronized to external optoelectronics systems or to other lasers. Particularly the synchronization of passively mode-locked laser sources to external clocks is attractive, since it implies the possibility of obtaining a femtosecond timing accuracy, as verified by early work in this area [143, 144]. Recently, detailed analysis of the sources of timing noise was provided by Haus and Mecozzi [145], and experimental verification was given by Spence et al. [146] in Ti:sapphire lasers and by Namiki et al. [147] in Er fiber lasers, where nearly quantum-limited timing jitter was obtained.

But whereas the synchronization of lasers to electronic clocks is of vital importance to most conventional telecommunications systems, applications in ultrafast optics typically call for the synchronization of two lasers in a master–slave configuration. A timing accuracy of around 5 ps has been obtained from such systems based on Er-doped fiber lasers [148, 149]. In [148] a low timing jitter was obtained by implementing a high-bandwidth cavity adjustment system based on an acousto-optic modulator in conjunction with a dispersive delay line. In [149] a low timing jitter was achieved by using two environmentally coupled fiber lasers.

In addition to simple master–slave configurations in which a fixed phase relation between two lasers is sought, time-resolved applications in ultrafast optics also call for an adjustable time delay. The conventional methods for implementing timing delay (moving mirrors, rotating glass blocks, etc.) are quite primitive, and they impose severe limitations on the attainable scan speed and range, which puts many types of measurements and applications out of the reach of ultrafast lasers. This difficulty has been partially circumvented by various implementations of asynchronous optical sampling, either between two lasers [150, 151] or between one laser and a free-running repetitive electrical waveform [152–154]. Free-running microwave signals with up to 150-GHz bandwidth have been detected in this fashion [154].

Many types of measurements, however, require two optical pulses, one pulse delayed with respect to the other, though this method of asynchronous optical sampling between two lasers suffers from a lack of adjustability. Because the scan range is set by the repetition period of the lasers, a required scan interval that is only a small subinterval of the pulse period is very wasteful of data acquisition time.

A method for overcoming these limitations has been demonstrated, i.e. a scanning temporal ultrafast delay (STUD) [155]. In this method the time delay between pulses from two mode-locked lasers can be electronically scanned at variable speeds in any subinterval of the pulse repetition period. The use of fiber lasers with ultrafast scanning delay lines is particularly attractive, as fiber lasers can operate at very low pulse repetition rates and with extremely low amplitude noise. When synchronizing lasers using electronic means, amplitude noise can cause timing errors via AM–PM conversion, although these effects can be minimized using chopper-stabilized phase detection [156]. However, for lasers passively mode-locked by nonlinear polarization evolution, it has been shown that all-optical limiting mechanisms [69] can be used for passive amplitude noise reduction [37].

5.1 Laser synchronization and “environmental coupling”

Synchronization of two ultrafast lasers is an essential capability for certain optical communications schemes and many types of measurements. In order to take advantage of the precise time resolution which is possible with ultrashort pulses, it is necessary in most cases to synchronize the two lasers with subpicosecond accuracy. Passive synchronization between two mode-locked lasers via a nonlinear optical interaction is the most accurate method, and several researchers have attained subpicosecond timing jitter between pairs of mode-locked lasers [157–162]. Hybrid optoelectronic methods have also been demonstrated (using optical cross-correlation) which give subpicosecond synchronization [163]. Electronic stabilization is somewhat less accurate, but allows the most versatility in timing adjustment. Two regeneratively mode-locked Ti:sapphire lasers have been electronically synchronized to within 2 ps [164], and commercial systems are now available for this purpose [165]. Here, we discuss experiments on electronic synchronization of two mode-locked fiber lasers. Since for most ultrafast time-resolved measurements, it is the relative timing delay between pulses that is important – and not the absolute timing with respect to some external reference – we concern ourselves mainly with the relative timing jitter between the two lasers rather than the absolute timing jitter of any one laser.

As is well known, variations in a laser’s environment (such as temperature, acoustic noise, and pump laser power) can cause fluctuations in the timing of the output pulses. The contribution of environmental effects to the relative timing jitter can be reduced by insuring that lasers experience the same perturbations. To this end an “environmentally coupled” twin fiber laser system, composed of master and slave lasers [149], was constructed as shown in Fig. 14. Both lasers were wound together (on a foam spool enclosed in packing foam), and they were pumped simultaneously by a single MOPA laser so that they experienced the same environmental and pump fluctuations. The two lasers had essentially identical cavity lengths, and had nominal repetition frequencies of $f_0 = 4.629$ MHz giving a “free temporal range” [151] of 217 ns. One end mirror of the slave laser was mounted on a PZT for dynamic cavity length adjustment. Co-wrapping the fiber lasers gives a factor-of-4 improvement in the relative versus absolute frequency drift over a period of several minutes. When the lasers were phase-locked, the timing jitter was found to be 5.4 ps root-mean-square RMS over

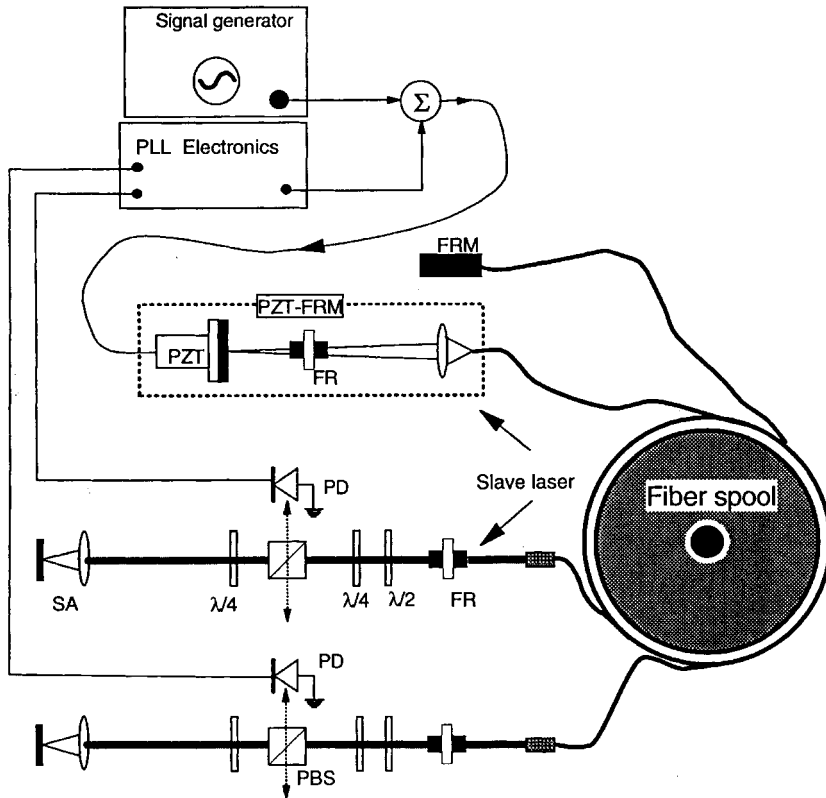


Fig. 14. Environmentally coupled, dual-fiber laser. Master and slave lasers are wrapped together on one spool. The master laser is terminated by a Faraday rotator mirror (FRM); the slave laser is terminated by a Faraday rotator mirror assembly (PZT-FRM) containing a PZT-mounted mirror. Other components are half-wave plate ($\lambda/2$), quarter-wave plate ($\lambda/4$), polarizing beamsplitter (PBS), Faraday rotator (FR), saturable absorber (SA), and photodiodes (PD-1 and PD-2)

a 3-min period, corresponding to a phase accuracy of one part in 40 000 or 30 arcs.

The timing accuracy achieved here demonstrates the benefits of co-packaging the two lasers. Another factor which contributed to the good stabilization is that the individual fiber lasers were very quiet, and exhibited amplitude fluctuations on the order of 0.1%, thus limiting the conversion of amplitude fluctuations into phase fluctuations. We also note that the RF phase detection in the phase locked loop PLL was at the fundamental repetition frequency, f_m , and not a higher harmonic. This allowed the pulse timing to be locked to any arbitrary point in the 217-ns free temporal range.

5.2 Electronically controlled scanning delay

Accurate synchronization of lasers is sufficient for some applications. However, many applications require that the time delay between two optical pulses be scanned controllably and accurately. The STUD technique [155] has allowed temporal scanning with selectable scan ranges (up to 10 ns) and selectable scanning frequencies (over 300 Hz).

The scanning laser method is based on the dual laser system described above. With the two lasers electronically synchronized, the slave laser cavity length, L_2 , is dithered about L_1 at a scan frequency f_{SCAN} (in the range of 30 Hz to 1 kHz) which is larger than the PLL bandwidth. This is done by applying the appropriate signal voltage to the PZT in addition to the feedback signal. This creates a time-varying delay between the pulses from the two lasers.

The time-varying pulse delay, $T_D(t)$, (defined as the relative time delay between the pulses from the two lasers), is proportional to the time integral of the cavity length mis-

match:

$$T_D(t) = T_0 + \frac{1}{L} \int_0^t \Delta L(t') dt'. \quad (9)$$

In a sense, this can be thought of as a “regenerative delay line”. If a square wave is applied to the slave laser PZT at a scanning frequency of f_{SCAN} , then this produces linear scanning of the time delay in both positive and negative directions for one-half of the scan cycle (i.e. a triangle wave). The scan range is $\Delta T_{max} = \Delta L_0 / 2L f_{SCAN}$, where ΔL_0 is the maximum displacement of the PZT. Various scan ranges and scan frequencies can be easily obtained by adjusting the signal generator in a straightforward way.

In order to use the rapid scanning technique for high accuracy measurements, it is also necessary to calibrate the scanning time delay scale with subpicosecond accuracy. This is possible even though the timing jitter of the synchronized dual laser system is 5 ps RMS. The calibration is accomplished by inserting a Fabry–Perot etalon into one beam in order to generate a series of evenly spaced calibration pulses, as shown in Fig. 15.

As a demonstration of the utility of this system, the temporal scanning and calibration techniques were used to measure carrier relaxation times in thin layers of InGaAs via a pump-probe technique as shown in Fig. 16. Pump pulses of 600 fs duration at 1550 nm excite carriers near the bandgap of the InGaAs. The transient absorption is probed at the same wavelength by 600-fs pulses from the slave laser. Figure 16 shows the transient absorption of a sample of InGaAsP (0.75 microns thick) measured over a 7-ns time interval (scanned at 30 Hz).

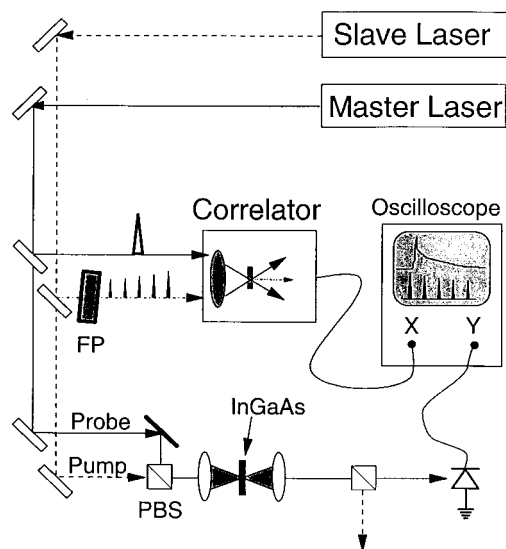


Fig. 15. Pump-probe measurement using scanning laser system and timing calibration method. A Fabry-Perot etalon (FP) generates the pulse train for timing calibration

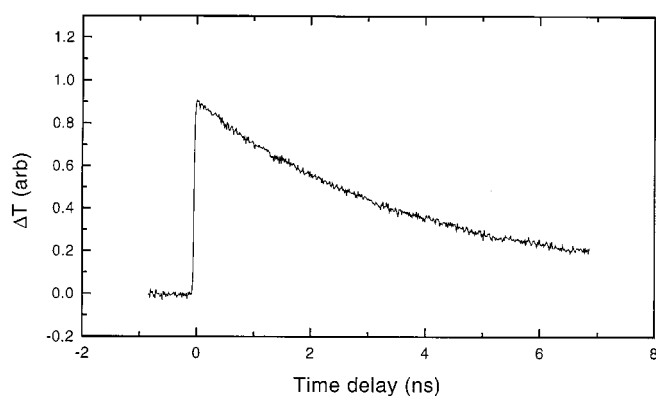


Fig. 16. Differential transmission signal near the band edge of intrinsic InGaAsP obtained when using a scanning temporal ultrafast delay based on two femtosecond fiber lasers

Although none of the rapid scanning methods demonstrated to date can match the accuracy of stepper-motor-driven delay lines, the STUD method greatly exceeds the performance of conventional scanning delays in many respects. Fiber lasers provide the additional advantage of putting a large time delay in a small package. For the 5-MHz laser, up to 200 ns of time delay is available, and in principle, any subinterval of that range can be scanned. Also, it should be mentioned that passively mode-locked lasers allow the simplest implementation of this method, although it could in principle be applied to actively mode-locked and regeneratively mode-locked lasers. This dual laser system and calibration method comprise a versatile, fast-scanning, ultrafast measurement system.

6 Summary

Over the last few years fiber lasers have been firmly established in the field of ultrafast optics. Though this paper could not describe all the advances that have been made, it was in-

tended to provide a cross-section of the work and to describe some of the most interesting applications. A limit imposed on the scope of the material covered was that we mainly concentrated on work on ultrafast pulse sources using optical fiber amplifiers. On the other hand great advancements have also been achieved in ultrafast optical processing using optical amplifiers. Ultrafast signal-processing techniques are now being routinely used in ultra-high-speed optical telecommunications and also require versatile fiber-based pulse sources. The ever growing number of applications of ultrafast optics in many fields will ensure a continued growth of research activities in the field of ultrafast fiber lasers.

Acknowledgements. We acknowledge M. Hofer, J.D. Minelly, M.A. Arbore, and M. Feyer for countless discussions and many critical contributions to this work.

References

1. A.M. Johnson, C.V. Shank: In *The Supercontinuum Laser Source*, ed. by R.R. Alfano (Springer, 1989)
2. A. Hasegawa, F.D. Tappert: *Appl. Phys. Lett.* **23**, 142 (1973)
3. L.F. Mollenauer, R.H. Stolen, J.P. Gordon: *Phys. Rev. Lett.* **45**, 1095 (1980)
4. J.R. Taylor: *Optical Solitons – Theory and Experiment* (Cambridge University Press, Cambridge, 1992)
5. G.P. Agrawal: *Nonlinear Fiber Optics* (Academic Press, San Diego, 1989)
6. A. Hasegawa: *Optical Solitons in fibers* (Springer Berlin, 1989)
7. S.B. Poole, D.N. Payne, M.E. Fermann: *Electron. Lett.* **21**, 737 (1985)
8. S.B. Poole, J.E. Townsend, D.N. Payne, M.E. Fermann, G.J. Cowle, R.I. Laming, P.R. Morkel: *J. Lightwave Tech.* **7**, 1989, (1224)
9. D.S. Funk, J.W. Carlson, J.G. Eden: *Electron. Lett.* **30**, 1859 (1994)
10. J. Schneider: *Electron. Lett.* **31**, 1250 (1995)
11. R.J. Mears, L. Reekie, I.M. Jauncey, D.N. Payne: *Electron. Lett.* **23**, 1026 (1987)
12. E. Desurvire, J.R. Simpson, P.C. Becker: *Opt. Lett.* **12**, 888 (1987)
13. E. Desurvire: *Erbium-Doped Fiber Amplifiers* (J. Wiley, New York, 1994)
14. I.N. Duling: *Compact Sources of Ultrashort Pulses* (Cambridge University Press, Cambridge 1995)
15. M.E. Fermann, M. Hofer, F. Haberl, A.J. Schmidt, L. Turi: *Opt. Lett.* **16**, 244 (1991)
16. M. Hofer, M.E. Fermann, F. Haberl, M.H. Ober, A.J. Schmidt: *Opt. Lett.* **16**, 502 (1991)
17. I.N. Duling III: *Opt. Lett.* **16**, 539 (1991)
18. K. Tamura, J. Jacobson, E.P. Ippen, H.A. Haus: *Opt. Lett.* **18**, 220 (1993)
19. M. Zirngibl, L.W. Stulz, J. Stone, J. Hugi, D. DiGiovanni, P.B. Hansen: *Electron. Lett.* **27**, 1734 (1991)
20. E.A. DeSouza, M.N. Islam, C.E. Socolich, W. Pleibel, R.H. Stolen, J.R. Simpson, D.J. DiGiovanni: *Electron. Lett.* **29**, 447 (1993)
21. D.E. Spence, P.N. Kean, W. Sibbett: *Opt. Lett.* **14**, 42 (1991)
22. W.S. Pelouch, P.E. Powers, C.L. Tang: *Opt. Lett.* **17**, 1070 (1992)
23. D. Strickland, G. Mourou: *Opt. Comm.* **56**, 219 (1985)
24. J. Squier, F. Salin, G. Mourou, D. Harter: *Opt. Lett.* **16**, 324 (1991)
25. S. Backus, J. Peatross, C.P. Huang, M.M. Murnane, H.C. Kapteyn: *Opt. Lett.* **20**, 2000 (1995)
26. M.E. Fermann: *Appl. Phys. B* **58**, 197 (1994)
27. D. Tavernier, D.J. Richardson, L. Dong, J.E. Caplen, K. Williams, R.V. Pentz: *Opt. Lett.* **22**, 378 (1997)
28. W.J. Miniscalco, *J. Lightwave Tech.* **9**, 234 (1991)
29. B. Desthieux, R.I. Laming, D.N. Payne: *Appl. Phys. Lett.* **63**, 586 (1993)
30. A. Galvanauskas, M.E. Fermann, P. Blixt, J.A. Tellefsen Jr., D. Harter: *Opt. Lett.* **19**, 1043 (1994)
31. A. Galvanauskas: *SPIE Proc.* **2377**, 117 (1995)
32. H. Zellmer, U. Willamowski, A. Tünnermann, H. Welling, S. Unger, V. Reichel, H.R. Müller, J. Kirchhoff, P. Albers: *Opt. Lett.* **20**, 578 (1995)
33. J.D. Kafka, T. Baer: *IEEE J. QE-24*, 341 (1988)

34. W. Koehner: *Solid-State Laser Engineering* (Springer Berlin, 1976)
35. R.G. Smith: *Appl. Opt.* **11**, 2489 (1972)
36. D.J. Richardson: Optical Society of America Annual Meeting, Rochester (1996), Paper MFF1
37. M.E. Fermann, D.H. Harter, J.D. Minelly, G.G. Vienne: *Opt. Lett.* **21**, 967 (1996)
38. M.J. Guy, D.U. Noske, A. Boskovic, J.R. Taylor: *Opt. Lett.* **19**, 828 (1994)
39. L.E. Nelson, K. Tamura, E.P. Ippen, H.A. Haus: *Opt. Soc. of Am. Conf. on Lasers and Electro-optics*, Baltimore, 238 (1995)
40. M.H. Hofer, M.H. Ober, R. Hofer, G.A. Reider, K. Sugden, I. Bennion, M.E. Fermann, G. Sucha, D.J. Harter, C.A. C. Mendonca, T.H. Chiu: *Opt. Soc. Am. Conf. on Optical Fiber Communication* (1996) Paper TuB3
41. S. Tsuda, W.H. Knox, J. Zyskind, J.E. Cunningham, W.Y. Jan, R. Pathak: *Opt. Soc. of Am. Conf. on Lasers and Electro-optics*, Anaheim, 494 (1996)
42. H.A. Haus, E.P. Ippen: *Opt. Lett.* **16**, 1331 (1991)
43. K. Tamura, L.E. Nelson, H.A. Haus, E.P. Ippen: *Appl. Phys. Lett.* **64**, 149 (1994)
44. M.H. Ober, M. Hofer, M.E. Fermann: *Opt. Lett.* **18**, 367 (1993)
45. L.E. Nelson, S.B. Fleischer, G. Lenz, E.P. Ippen: *Opt. Lett.* **21**, 1759 (1996)
46. M.E. Fermann, D. Harter, J.D. Minelly, G.G. Vienne: *Opt. Soc. of Am. Conf. on Lasers and Electro-optics*, Anaheim, 493 (1996)
47. M.E. Fermann, L.M. Yang, M.L. Stock, M.J. Andrejco: *Opt. Lett.* **19**, 43 (1994)
48. R.C. Sharp, D.E. Spock, N. Pan, J. Elliot: *Opt. Lett.* **21**, 881 (1996)
49. M.E. Ferman, K. Sugden, I. Bennion: *Opt. Lett.* **20**, 172 (1995)
50. R. Kashap: *Opt. Fibre Tech.*, **1**, 17 (1994)
51. M.E. Fermann, K. Sugden, I. Bennion: *Electron. Lett.* **31**, 194 (1995)
52. M. Hofer, M.H. Ober, R. Hofer, M.E. Fermann, G. Sucha, D. Harter, K. Sugden, I. Bennion, C.A. C. Mendonca, T. Chiu: *Opt. Lett.* **20**, 1701 (1995)
53. A.B. Grudinin, D.J. Richardson, D.N. Payne: *Electron. Lett.* **29**, 1860 (1993)
54. S. Gray, A.B. Grudinin, W.H. Loh, D.N. Payne: *Opt. Lett.* **20**, 189 (1995)
55. A.N. Pilipetskii, E.A. Golovchenko, C.R. Menyuk: *Opt. Lett.* **20**, 907 (1995)
56. S. Gray, A.B. Grudinin: *Opt. Lett.* **21**, 207 (1996)
57. M.E. Fermann, J.D. Minelly: *Opt. Lett.* **21**, 970 (1996)
58. S. Gray, A.B. Grudinin: *Opt. Soc. of Am. Conf. on Lasers, Electro-optics*, 494, Anaheim (1996)
59. B.C. Collings, K. Bergmann, S. Tsuda, W.H. Knox: to be presented at *Opt. Soc. of Am. Conf. on Lasers and Electro-optics*, Baltimore (1997)
60. J.D. Kafka, T. Baer, D.W. Hall: *Opt. Lett.* **14**, 1269 (1989)
61. M. Hofer, M.E. Fermann, F. Haberl, J.E. Townsend: *Opt. Lett.* **15**, 1467 (1990)
62. M.E. Fermann, M. Hofer, F. Haberl: *Electron. Lett.* **26**, 1737 (1990)
63. F.X. Kärtner, D. Kopf, U. Keller, J. Opt. Soc. Am. B **12**, 486 (1995)
64. F.X. Kärtner, U. Keller: *Opt. Lett.* **20**, 16 (1995)
65. D.H. Kuizenga, A.E. Siegman: *IEEE J. QE-6*, 694 (1970)
66. M. Nakazawa, K. Tamura, E. Yoshida: *Electron. Lett.* **32**, 461 (1996)
67. T.F. Carruthers, I.N. Duling III: *Opt. Lett.* **21**, 1927 (1996)
68. D.J. Jones, H.A. Haus, E.P. Ippen: *Opt. Lett.* **21**, 1818 (1996)
69. C.R. Doerr, H.A. Haus, E.P. Ippen, M. Shirasaki, K. Tamura: *Opt. Lett.* **19**, 31 (1994)
70. A. Baltuska, Z. Wei, M.S. Pshenichnikov, D.A. Wiersma: *Opt. Lett.* **22**, 102 (1997)
71. W.H. Tomlinson, R.H. Stolen, C.V. Shank, J. Opt. Soc. Am. B **1**, 139 (1984)
72. J.A. R. Williams, I. Bennion, L. Zhang: *IEEE Photon. Tech. Lett.* **7**, 491 (1995)
73. K. Tamura, T. Komukai, T. Yamamoto, T. Imai, E. Yoshida, M. Nakazawa: *Electron. Lett.* **31**, 2194 (1995)
74. K. Tamura, M. Nakazawa: *Opt. Lett.* **21**, 68 (1996)
75. T. Morioka, K. Mori, M. Saruwatari: *Electron. Lett.* **29**, 862 (1993)
76. T. Morioka, S. Kawanishi, K. Mori, M. Saruwatari: *Electron. Lett.* **30**, 1166 (1994)
77. T. Morioka, K. Okamoto, M. Ishii, M. Saruwatari: *Electron. Lett.* **32**, 836 (1996)
78. M.N. Islam, G. Sucha, I. Bar-Joseph, M. Wegener, J.P. Gordon, D.S. Chemla: *Opt. Lett.* **14**, 370 (1989)
79. S. Kawanishi, H. Takara, T. Morioka, O. Kamatani, M. Saruwatari, *Electron. Lett.* **31**, 816 (1995)
80. K. Kurokawa, M. Nakazawa: *Appl. Phys. Lett.* **58**, 2871 (1991)
81. I.Y. Khurshev, A.B. Grudinin, E.M. Dianov, D.V. Korobkin, V.A. Semenov, A.M. Prokhorov: *Electron. Lett.* **26**, 456 (1990)
82. D.J. Richardson, V.V. Afanasjev, A.B. Grudinin, D.N. Payne: *Opt. Lett.* **17**, 1596 (1992)
83. S.V. Chernikov, E.M. Dianov, D.J. Richardson, D.N. Payne: *Opt. Lett.* **18**, 476 (1993)
84. D.J. Richardson, A.G. Grudinin, D.N. Payne: *Electron. Lett.* **28**, 778 (1992)
85. P.V. Mamyshev, S.V. Chernikov: *Opt. Lett.* **15**, 1076 (1990)
86. M. Nakazawa, E. Yoshida, Y. Kimura: *Electron. Lett.* **30**, 2038 (1994)
87. K. Tamura, E. Yoshida, E. Yamada, M. Nakazawa: *Electron. Lett.* **32**, 835 (1996)
88. K. Tamura, E. Yoshida, M. Nakazawa: *Electron. Lett.* **32**, 1691 (1996)
89. E.A. Swanson, S.R. Chinn, K. Hall, K.A. Rauschenbach, R.S. Bondurant, J.W. Miller: *IEEE Photon. Tech. Lett.*, **6**, 1194 (1994)
90. E.A. Swanson, S.R. Chinn: *IEEE Photonics Techn. Lett.*, **7**, 114 (1995)
91. M.J. Guy, S.V. Chernikov, J.R. Taylor, D.G. Moodie, R. Kashap, *Electron. Lett.* **31**, 740 (1995)
92. P.V. Mamyshev, S.V. Chernikov, E.M. Dianov: *IEEE J. QE-27*, 2347 (1991)
93. S.V. Chernikov, J.R. Taylor, P.V. Mamyshev, E.M. Dianov, *Electron. Lett.* **28**, 931 (1992)
94. S.V. Chernikov, D.J. Richardson, R.I. Laming, E.M. Dianov, D.N. Payne, *Electron. Lett.* **28**, 1210 (1992)
95. J.T. Ong, R. Takashii, M. Tsuchiya, S.H. Wong, R.T. Sahara, Y. Ogawa, T. Kamiya: *IEEE J. QE-29*, 1701 (1993)
96. K.A. Ahmed, H.H. Y. Cheng, H.F. Liu: *Electron. Lett.* **31**, 195 (1995)
97. P.K. Cheo, L. Wang, M. Ding: *IEEE Photon. Techn. Lett.* **8**, 66 (1996)
98. F. Fontana, L. Bossalini, P. Franco, M. Midrio, M. Romagnoli, S. Wabnitz: *Electron. Lett.* **30**, 321 (1994)
99. M. Romagnoli, S. Wabnitz, P. Franco, M. Midrio, F. Fontana and G.E. Town, *J. Opt. Soc. Am. B* **12**, 72 (1995)
100. D. O Culverhouse, D.J. Richardson, T.A. Birks, P. St. J. Russell: *Opt. Lett.* **20**, 2381 (1995)
101. M.Y. Jeon, H.K. Lee, K.H. Kim, E.H. Lee, S.H. Yun, B.Y. Kim, Y.W. Koh: *IEEE Photonics Techn. Lett.* **8**, 1618 (1996)
102. A. Galvanauskas, P. Blixt, J.A. Tellefson Jr.: *Appl. Phys. Lett.* **63**, 1742 (1993)
103. M. Shell, D. Huhse, D. Bimberg: *Appl. Phys. Lett.* **64**, 1923 (1994)
104. A. Galvanauskas, P.A. Krug, D. Harter: *Opt. Lett.* **21**, 1049 (1996)
105. M. Schell, D. Bimberg, V.A. Bogatyryov, E.M. Dianov, A.S. Kurkov, V.A. Semenov, A.A. Sysoliatin: *IEEE Photon. Tech. Lett.*, **6**, 1191 (1994)
106. D.J. Richardson, R.P. Chamberlain, L. Dong, D.N. Payne, *Electron. Lett.* **30**, 1326 (1994)
107. A.B. Grudinin, D.J. Richardson, R.P. Chamberlin, L. Dong, D.N. Payne: *Optical Fiber Conf.*, *Opt. Soc. of America Tech. Digest Series* **4**, 91 (1994)
108. D.M. Pataca, M.L. Rocha, R. Kashap, K. Smith: *Electron. Lett.* **31**, 35 (1995)
109. M. Nakazawa, K. Suzuki: *Electron. Lett.* **31**, 1084 (1995)
110. M. Nakazawa, K. Suzuki: *Electron. Lett.* **31**, 1076 (1995)
111. C.P. Barty, T. Guo, C. Le Blanc, F. Raksi, C. Rose-Petruck, J.A. Squier, K.R. Wilson, V.V. Yakovlev, K. Yamakawa: *SPIE Proc.* **2701**, 85 (1996)
112. A. Galvanauskas, M.E. Fermann, D. Harter: *Opt. Lett.* **19**, 1201 (1994)
113. A. Galvanauskas, M.E. Fermann, D. Harter, K. Sugden, I. Bennion: *Appl. Phys. Lett.* **66**, 1053 (1995)
114. J. Nilsson, B. Jaskorzynska: *Opt. Lett.* **18**, 2099 (1993)
115. M.D. Perry, T. Ditmire, B.C. Stuart: *Opt. Lett.* **19**, 2149 (1994)
116. M.J. Adams: *An Introduction to Optical Waveguides* (J. Wiley, New York 1981)
117. D. Taverner, A. Galvanauskas, D. Harter, D.J. Richardson, and L. Dong: *Conf. on Lasers and Electro-optics: Opt. Soc. Am. Technical Digest Series* **9**, 496 (1996)
118. O.E. Martinez: *IEEE J. QE-23*, 59 (1987)
119. E.B. Treacy: *IEEE J. QE-5*, 454 (1969)
120. C.P. Barty, G. Korn, F. Raksi, C. Rose-Petruck, J. Squier, A.-C. Tien, K.R. Wilson, V.V. Yakovlev, K. Yamakawa: *Opt. Lett.* **21**, 219 (1996)
121. W.E. White, F.G. Patterson, R.L. Combs, D.F. Price, R.L. Shepherd: *Opt. Lett.* **18**, 1343 (1993)
122. J.D. Minelly, A. Galvanauskas, D. Harter, J.E. Caplen, L. Dong: to be presented at *Opt. Soc. Am. Conf. on Lasers and Electro-optics*, Baltimore (1997)

123. E. Snitzer, H. Po, F. Hakimi, R. Tumminelly, B.C. McCollum: Optical Fiber Sensors: Opt. Soc. Am. Technical Digest Series **1** (1988), Paper PD5
124. D.J. Ripin, L. Goldberg: Electron. Lett. **31**, 2204 (1995)
125. L. Dong, M.J. Cole, A.D. Ellis, M. Durkin, M. Ibsen, V. Gusmeroli, R.I. Laming: Optical Fiber Communication Conf., Dallas (1997), Paper PD6
126. A. Galvanauskas, D. Harter, S. Radic, G.P. Agrawal, Conf. on Lasers and Electro-optics: Opt. Soc. Am. Technical Digest Series **9**, 499 (1996)
127. P.J. Lemaire, R.M. Atkins, V. Mizrahi, W.A. Reed: Electron. Lett. **29**, 1191 (1993)
128. G. Meltz, W.W. Morey, W.H. Glenn: Opt. Lett. **14**, 823 (1989)
129. K.O. Hill, B. Malo, F. Blodeau, D.C. Johnson, J. Albert, Appl. Phys. Lett. **62**, 1035 (1993)
130. A. Galvanauskas, M.E. Fermann, D. Harter, J.D. Minelly, G.G. Vienne, J.E. Caplen, in Conference on Lasers and Electro-Optics: Opt. Soc. Am. Technical Digest Series **9**, 495 (1996)
131. M.A. Arbore, M.M. Fejer, M.E. Fermann, A. Hariharan, A. Galvanauskas, D. Harter: Opt. Lett. **22**, 13 (1997)
132. G.D. Boyd, D.A. Kleinman, J. Appl. Phys. **39**, 3597 (1968)
133. M. Yamada, N. Nada, M. Saitoh, K. Watanabe: Appl. Phys. Lett. **62**, 436 (1993)
134. K. Mizuuchi, K. Yamamoto: Opt. Lett. **21**, 107 (1996)
135. L.E. Myers, R.C. Eckardt, M.M. Fejer, R.L. Byer, W.R. Bosenberg, J.W. Pierce, J. Opt. Soc. Am. B **12**, 2102 (1995)
136. S.A. Akhmanov, A.P. Sukhorukov, A.S. Chirkin, Soviet Phys. JETP, **28**, 748 (1969)
137. D.C. Edelstein, E.S. Wachman, C.L. Tang: Appl. Phys. Lett. **54**, 1728 (1989)
138. R. Danielius, A. Piskarskas, A. Stabinis, G.P. Banfi, P. Di Trapani, and R. Righini, J. Opt. Soc. Am. B **10**, 2222 (1993)
139. M.K. Reed, M.K. Steiner-Sheoard, M.S. Armas, D.K. Negus, J. Opt. Soc. Am. B **12**, 2229 (1995)
140. A. Galvanauskas, M.A. Arbore, M.M. Fejer, M.E. Fermann, D. Harter: Opt. Lett. **22**, 105 (1997)
141. L.E. Myers, R.C. Eckardt, M.M. Fejer, R.L. Byer, W.R. Bosenberg: Opt. Lett. **21**, 591 (1996)
142. G.P. Banfi, C. Solcia, P. Di Trapani, R. Danielius, A. Piskarskas, R. Righini, R. Torre: Opt. Commun. **118**, 353 (1995)
143. M. Hofer, M.H. Ober, F. Haberl, M.E. Fermann: IEEE J. QE-**28**, 720 (1992)
144. F. Haberl, M.H. Ober, M. Hofer, M.E. Fermann, E. Wintner, A.J. Schmidt: IEEE Photon. Tech. Lett. **3**, 1071 (1991)
145. H.A. Haus, A. Mecozzi: IEEE J. QE-**29**, 983 (1993).
146. D.E. Spence, J.M. Dudley, K. Lamb, W.E. Sleat, W. Sibbett: Opt. Lett. **19**, 481 (1994).
147. S. Namiki, C.X. Yu, H.A. Haus, JOSA B **13**, 2817 (1996).
148. M. Jiang, W. Sha, L. Rahman, B.C. Barnett, J.K. Anderson, M.N. Islam, K.V. Reddy: Opt. Lett. **21**, 809 (1996)
149. G. Sucha, M. Hofer, M.E. Fermann, F. Haberl, D. Harter: Opt. Lett. **21**, 1570 (1996)
150. J.D. Kafka, J.W. Pieterse, M.L. Watts: Opt. Lett., **17**, 1286 (1992)
151. R.J. Kneisler, F.E. Lytle, G.J. Fiechtner, Y. Jiang, G.B. King, N.M. Laurendeau: Opt. Lett. **14**, 260 (1989)
152. A. Black, R.B. Apte, D.M. Bloom, Rev. Sci. Instr. **63**, 3191 (1992)
153. K.S. Giboney, S.T. Allen, M.J. W. Rodwell, J.E. Bowers: IEEE Photon. Tech. Lett. **6**, 1353 (1994)
154. T. Löffler, T. Pfeifer, H.G. Roskos, H. Durz, D.W. van der Weide: Microelectronic Engineering **31**, 397 (1996)
155. G. Sucha, M.E. Fermann, D. Harter, M. Hofer: IEEE J. Quantum Electron. (in press)
156. M.J. W. Rodwell, D.M. Bloom, K.J. Weingarten: IEEE J. Quantum Electron., QE-**25**, 817 (1989)
157. J.M. Evans, D.E. Spence, D. Burns, W. Sibbett: Opt. Lett. **13**, 1074 (1993)
158. M.R. X. de Barros, P.C. Becker: Opt. Lett. **18**, 631 (1993)
159. D.R. Dykaar, S.B. Darak: Opt. Lett. **18**, 634 (1993)
160. Z. Zhang, T. Yagi: Opt. Lett. **18**, 2126 (1993)
161. D.A. Pattison, P.N. Kean, J.W.D. Gray, I. Bennion, N.J. Doran, IEEE Photon. Tech. Lett. **7**, 1415 (1995)
162. W.H. Knox, F.A. Beisser: Opt. Lett. **17**, 1012 (1992).
163. S.P. Djaili, J.S. Smith, A. Dienes: Appl. Phys. Lett. **55**, 418 (1989).
164. D.E. Spence, W.E. Sleat, J.M. Evans, W. Sibbett, J.D. Kafka, Opt. Comm. **101**, 286 (1993)
165. Spectra Physics Lok-to-Clock™ system